The Electron Neutrino Mass Measurement by the HOLMES experiment

A Status Report

Andrea Giachero

on behalf of HOLMES collaboration

University and INFN of Milano Bicocca

November 24, 2015

xs

HOLMES

Known facts

- Neutrino are fermions;
- There are 3 active neutrino flavors (ν_e, ν_μ, ν_τ);
- Neutrino flavor states are mixture of mass states (ν_1, ν_2, ν_3);

$$\Rightarrow \text{neutrino oscillation}$$

$$\Downarrow$$

$$\delta m^2_{ij} = |m^2_i - m^2_j|$$

$$\sin^2\theta_{ij} = f(|U_{ij}|^2)$$

Parameter	Best fit	1σ range	$\sigma_{\text{symmetric}}$
$\mathcal{NH}$			
$\sin^2(\theta_{12})$	$3.08 \cdot 10^{-1}$	$(2.91 - 3.25) \cdot 10^{-1}$	$0.17 \cdot 10^{-1}$
$\sin^2(\theta_{13})$	$2.34 \cdot 10^{-2}$	$(2.16 - 2.56) \cdot 10^{-2}$	$0.22 \cdot 10^{-2}$
δm^2 [eV^2]	$7.54 \cdot 10^{-5}$	$(7.32 - 7.80) \cdot 10^{-5}$	$0.26 \cdot 10^{-5}$
Δm^2 [eV^2]	$2.44 \cdot 10^{-3}$	$(2.38 - 2.52) \cdot 10^{-3}$	$0.08 \cdot 10^{-3}$
$\mathcal{IH}$			
$\sin^2(\theta_{12})$	$3.08 \cdot 10^{-1}$	$(2.91 - 3.25) \cdot 10^{-1}$	$0.17 \cdot 10^{-1}$
$\sin^2(\theta_{13})$	$2.39 \cdot 10^{-2}$	$(2.18 - 2.60) \cdot 10^{-2}$	$0.21 \cdot 10^{-2}$
δm^2 [eV^2]	$7.54 \cdot 10^{-5}$	$(7.32 - 7.80) \cdot 10^{-5}$	$0.26 \cdot 10^{-5}$
Δm^2 [eV^2]	$2.40 \cdot 10^{-3}$	$(2.33 - 2.47) \cdot 10^{-3}$	$0.07 \cdot 10^{-3}$

Results of the global 3ν oscillation analysis [1, 2]

$$\begin{cases} \delta m^2 = m_2^2 - m_1^2 \\ \Delta m^2 = m_3^2 - \dfrac{m_1^2 + m_2^2}{2} \end{cases}$$

$$|\nu_\alpha\rangle = \sum_j U_{\alpha j} |\nu_j\rangle$$

$$\begin{cases} |\nu_\alpha\rangle & : \text{Flavor weak eigenstate;} \\ U_{\alpha j} & : \text{Neutrino mixing matrix;} \\ |\nu_j\rangle & : \text{Mass eigenstate.} \end{cases}$$

Parameter	Dominated by [1]
θ_{12}	Solar data
θ_{13}	Short-baseline (SBL) reactor data Daya Bay, RENO
θ_{23}	Atmospheric data Super-Kamiokande
δm^2	Long-baseline (LBL) accelerator data KamLAND
Δm^2	Long-baseline (LBL) accelerator data MINOS, T2K

Neutrino mass hierarchy

Unknown facts

- Mass scale:
  - Mass of the lightest neutrino
- Mass ordering (hierarchy):
  - degenerate ($\mathcal{QD}$): $m_1 \simeq m_2 \simeq m_3$
  - normal ($\mathcal{NH}$) : $m_1 \ll (<) m_2 \ll m_3$
  - inververd ($\mathcal{IH}$) : $m_3 \ll m_1 \lesssim m_2$
- Mass Nature:
  - Dirac particle : $\nu \neq \overline{\nu}$
  - Majorana particle: $\nu = \overline{\nu}$
- Others?

Oscillations experiments:

- Sensitive ONLY to the squared mass differences: δm^2_{ij};
- NO information about absolute mass scale and nature.

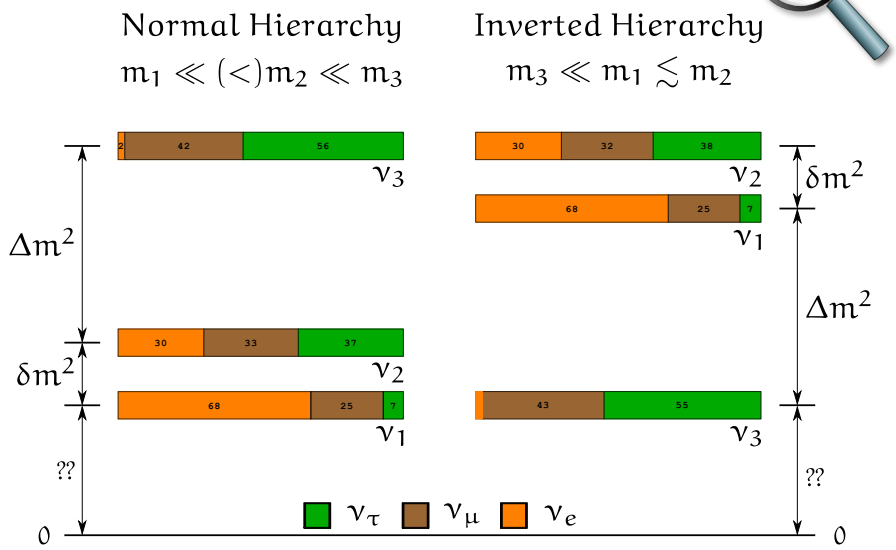

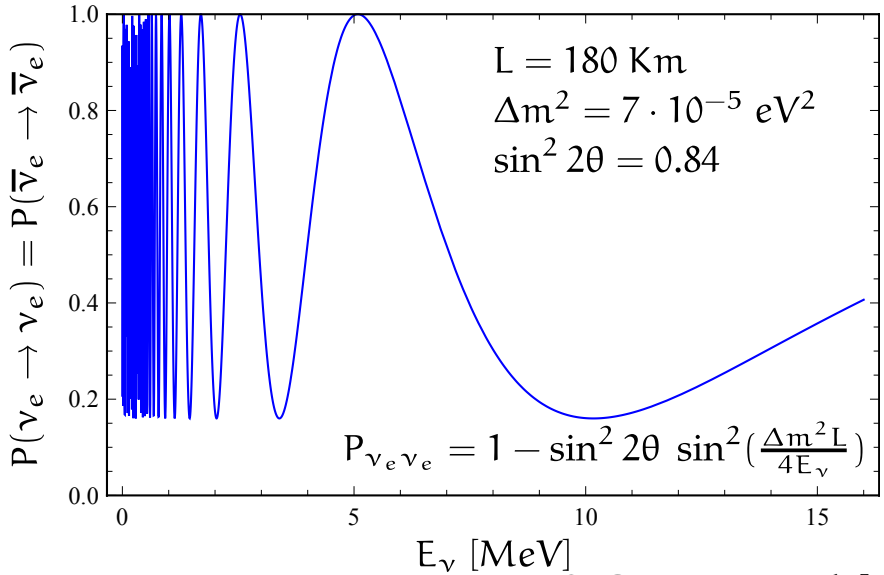

S. Goswami *et al.* [3]

Neutrino mass: available experimental tools

Constraint from cosmology:

- Cosmic microwave background (CMB);
- Galaxy clustering;
- Lyman-alpha forest;
- Weak lensing.

Observable	$m_\Sigma = \sum_k m_{\nu_k}$
Best limit	$m_\Sigma \leqslant 0.23$ eV @ 95% [4]

Constraint from the Neutrinoless Double Beta-Decay ($0\nu\beta\beta$):

- Forbidden by Standard Model ($\Delta L = 2$);
- Allowed only for Majorana neutrino;
- Never observed.
- $\left[\tau^{0\nu}_{1/2}\right]^{-1} = G^{0\nu}\left|M^{0\nu}\right|^2\left|\langle m_{\beta\beta}\rangle\right|^2$

Decay	$(A, Z) \rightarrow (A, Z+2) + 2e^-$
Observable	$m_{\beta\beta} = \left\|\sum_k m_{\nu_k} U^2_{ek}\right\|$
Best limit	$m_{\beta\beta}(^{76}\mathrm{Ge}) \leqslant (200 \div 400)$ meV [5] $m_{\beta\beta}(^{136}\mathrm{Xe}) \leqslant (190 \div 450)$ meV [6]

$m_{\beta\beta}$: Effective Majorana Mass

Constraint from the Direct Neutrino Mass Determination:

- Kinematical analysis of the end point region of the β decay spectra;
- The neutrino is not directly observed but the energy of the decay products is precisely measured;

Decay	$(A, Z) \rightarrow (A, Z+1) + e^- + \overline{\nu}_e$ (βD) $(A, Z) + e^- \rightarrow (A, Z-1) + \nu_e$ (EC)
Observable	$m_\beta = \sqrt{\sum_k m^2_{\nu_k}\left\|U_{ek}\right\|^2}$
Best limit	$m_\beta \leqslant 2.2$ eV [7, 8]

Neutrino mass: available experimental tools (cont.)

HOLMES

Tool	Cosmology	Double Beta Decay	Beta Decay End Point
Observable	$m_\Sigma = \sum_k m_{\nu_k}$	$m_{\beta\beta} = \lvert\sum_k m_{\nu_k} U_{ek}^2\rvert$	$m_\beta = \sqrt{\sum_k m_{\nu_k}^2 \lvert U_{ek}\rvert^2}$
Present Sensitivity	$\simeq$ 0.1 eV	$\simeq$ 0.1 eV	2 eV
Future Sensitivity	0.01 eV	0.01 eV	0.2 eV
Model Dependency	yes ☹	yes ☹	no ☺
Systematics	large ☹	small ☺	large ☹

Cosmology

- The parameter m_Σ suffers of cosmological model dependency;

Neutrinoless Double Beta

- The calculations of nuclear matrix elements of $0\nu\beta\beta$-decay is a challenge for nuclear physics (several different approach, model dependency).

Beta Decay end-point measurement

- The measurement of the end point of nuclear beta or electron capture (EC) decays spectra is the only model-independent.

Direct neutrino mass measurements

Kinematics of weak decays with ν emission:

- only energy and momentum conservation;
- no further assumptions;
- low Q nuclear beta decays (^{3}H, ^{187}Re);

Two approaches with different:

- Spectrometry: the β source is outside the spectrometry detector;
- Calorimetry: the β source is contained in the calorimetry detector which measures all the energy released except the ν energy.

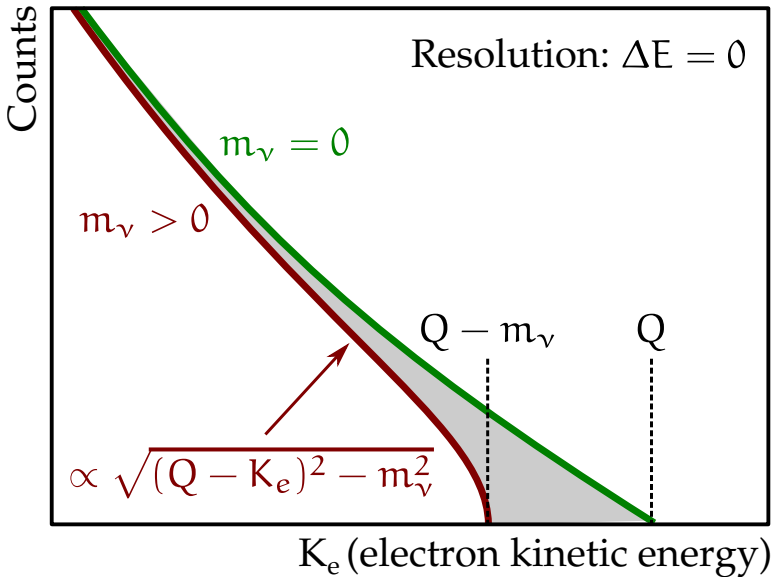

Spectrometry: KATRIN

Large MAC-E filter spectrometer with ^{3}H source

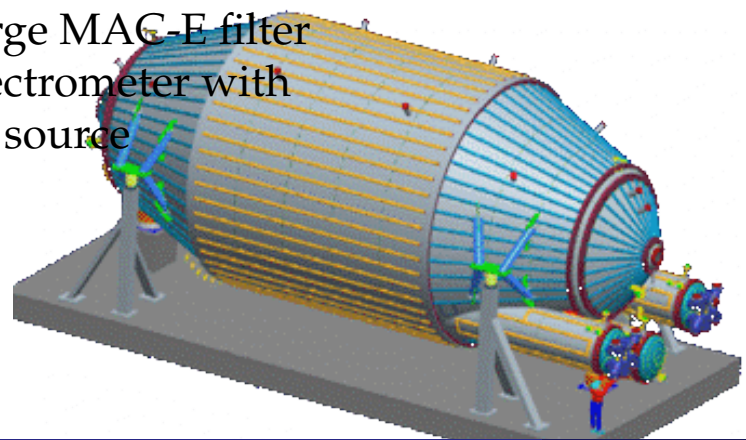

Calorimetry: Mare, ECHo, Holmes

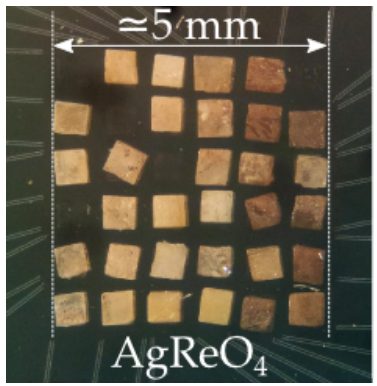

Array of low temperature microcalorimeters with ^{187}Re or ^{163}Ho

Experimental approaches

Spectrometers: source ≠ detector

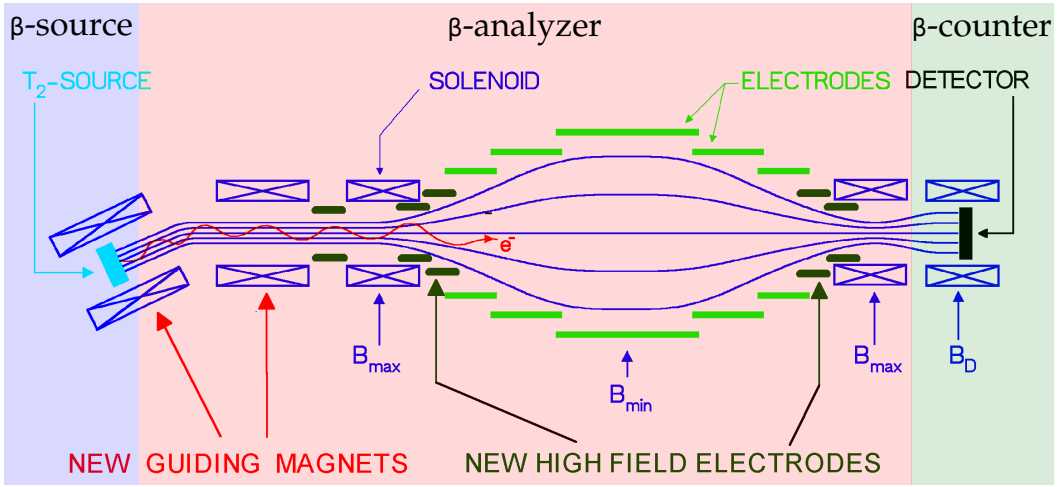

(Mainz spectrometer sketch-up from C. Kraus *et al.* [9])

- Tritium β decay: $^3\mathrm{H} \rightarrow ^3\mathrm{He}^+ + e^- + \overline{\nu}_e$
- Magnetic spectrometers and MAC-E filter [10];
- The β-electrons with enough energy to pass the MAC-E filter are detected;

Calorimeters: source ⊆ detector

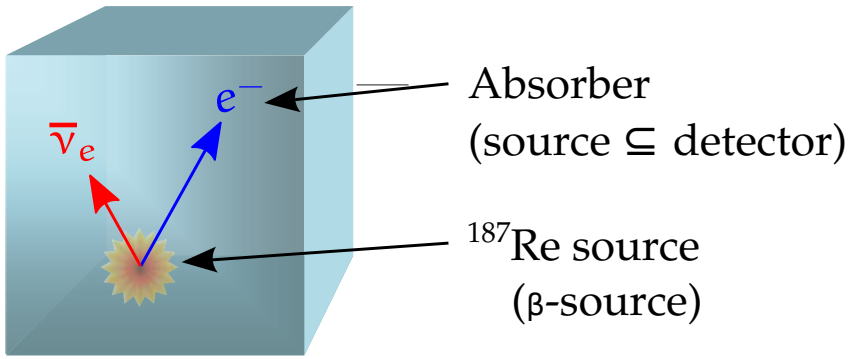

$$^{187}\mathrm{Re} \rightarrow ^{187}\mathrm{Os} + e^- + \overline{\nu}_e$$

- The β source is embedded in the detector (absorber);
- Ideally measurement of all the energy E released in the decay except for the ν_e energy;

Calorimeters vs Spectrometers

HOLMES

General experimental requirements:

- High statistics at the beta spectrum end-point:
  - Low end-point energy Q: $F(\delta E) \propto (\delta E/Q)^3$
    $\Rightarrow$ where δE is the energy range considered near the end point;
  - High source activity and high efficiency;
- High energy resolution ΔE (same order of magnitude of m_ν sensitivity);
- High signal-to-noise ratio (SNR);
- Small systematic effects.

Spectrometers: source $\neq$ detector:

- ☺ high statistics: $\tau_{1/2}(^3H) = 12.3$ y;
- ☺ high energy resolution: $\delta E \simeq 1$ eV;
- ☹ systematics due to source effect;
- ☹ systematics due to decay to excited states;
- ☹ background.

Calorimeters: source $\subseteq$ detector:

- ☺ no backscattering;
- ☺ no energy losses in the source;
- ☺ no solid state excitation;
- ☺ no atomic/molecular final state effect;
- ☹ limited statistics: $\tau_{1/2}(^{187}Re) \simeq 4 \cdot 10^{10}$ y;
- ☹ systematics due to pile-up;
- ☹ background.

Spectrometers: present results

Mainz Experiment: solid ^{3}H source (1997-2001)

$$m_\nu^2 = -0.6 \pm 2.2_{(stat)} \pm 2.1_{(sys)}\ eV^2$$

$$\Downarrow$$

$$m_\nu < 2.3\ eV\ (95\%\ C.L.)\ [8, 9]$$

Results after all critical systematics measured (atomic physics, surface and solid state physics, inelastic scattering, self-charging, neighbour excitation)

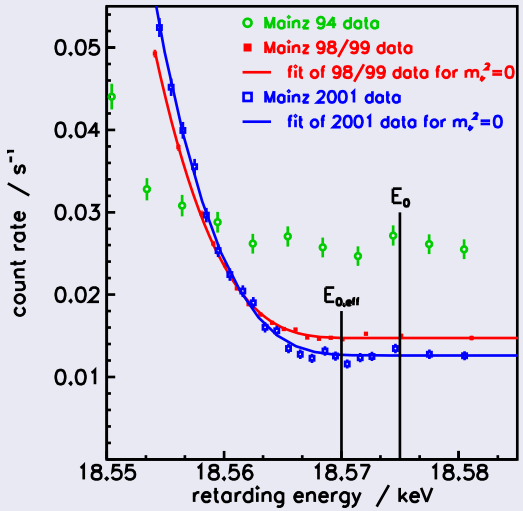

Troitsk Experiment: gaseous ^{3}H source (1997-2004)

$$m_\nu^2 = -0.67 \pm 1.89_{(stat)} \pm 1.68_{(sys)}\ eV^2$$

$$\Downarrow$$

$$m_\nu < 2.05\ eV\ (95\%\ C.L.)\ [7, 11]$$

Most significant systematics:

- Stability of source conditions;
- Energy loss inside tritium source;
- Background due to non-optimal vacuum;

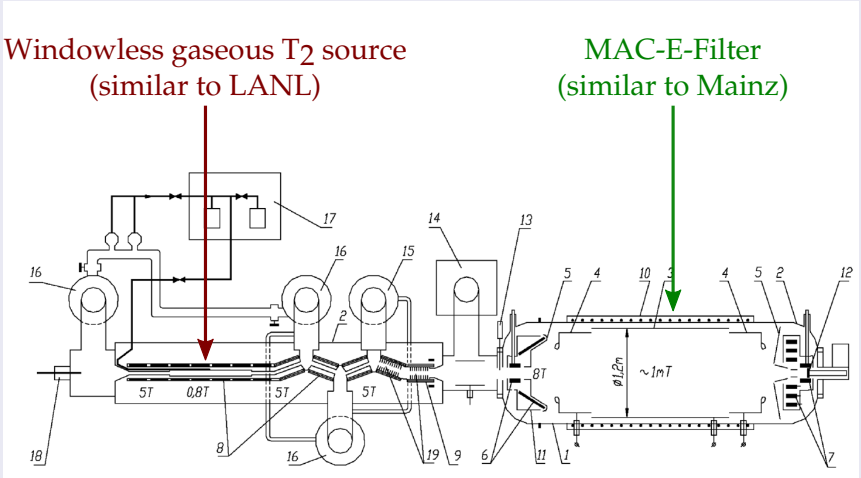

HOLMES

The KArlsruhe TRItium Neutrino Experiment (KATRIN)
@ KIT (Karlsruhe Institute of Technology)

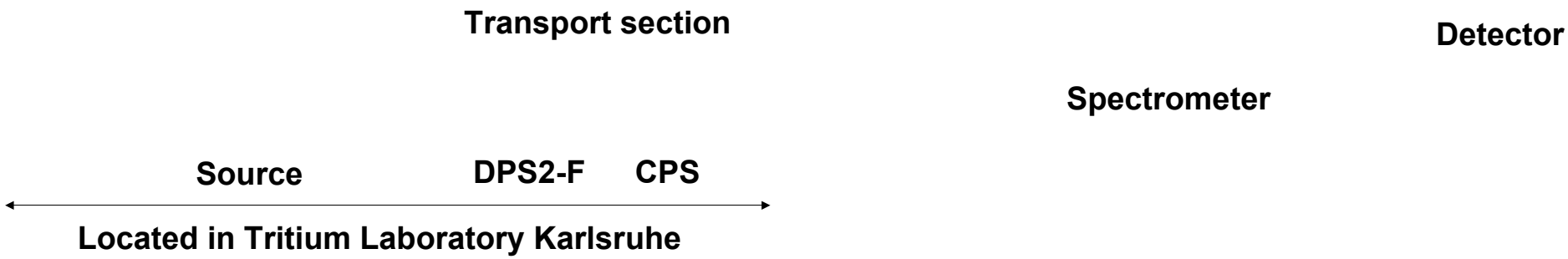

- Larger electrostatic spectrometer ever built (stainless steel vessel, $\varnothing = 10$ m , $L = 22$ m);
- Intense Windowless Gaseous Tritium Source (WGTS): 10^{11} β decay electrons per second;
- Energy resolution: $\Delta E = 0.93$ eV;
- High luminosity: $L = 20$ cm^2 (Troitsk: $L = 0.6$ cm^2);
- Ultrahigh vacuum requirements: $p < 10^{-11}$ mbar (to reduce the background).

Expected statistical sensitivity: $m_\nu < 0.2$ eV @ 90% C.L. [12, 13]

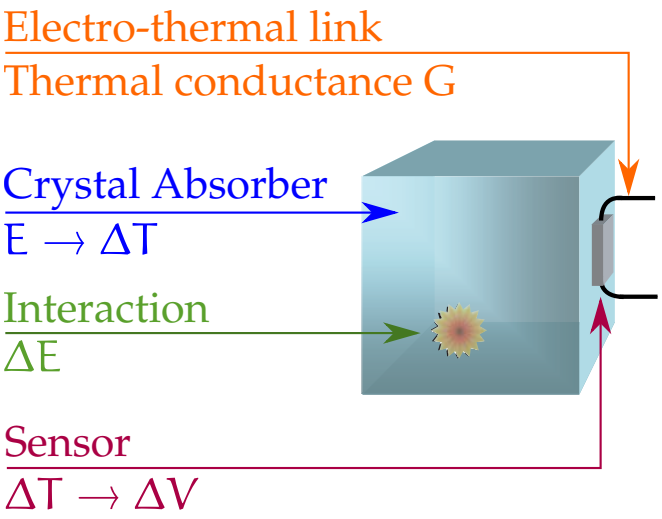

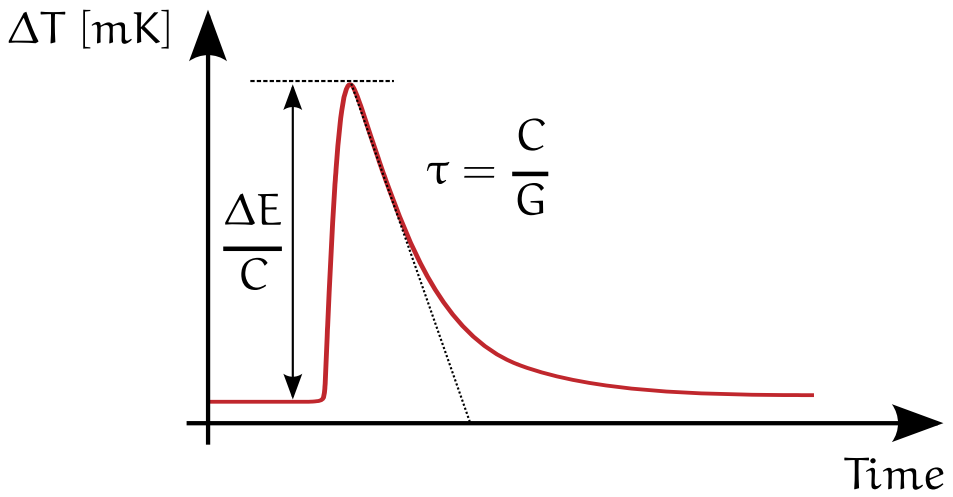

- Complete energy thermalization: ionization, excitation $\Rightarrow$ heat$\Rightarrow$calorimetry;
- $\Delta T = \frac{\Delta E}{C}$ where ΔE is the released energy and C the total thermal capacity;
  - Absorber with very low thermal capacity: $C \downarrow \quad \Rightarrow \quad \Delta T \uparrow$;
  - Debay low for superconductors below T_C and dielectric: $C \propto \left(\frac{T}{\Theta_D}\right)^3$;
  - A very low temperature is needed: $T \downarrow \Rightarrow C \downarrow \Rightarrow \Delta T \uparrow \Rightarrow (T = 10 \div 100\ \text{mK})$;
- Limit to energy resolution: statistical fluctuation of internal energy $\Delta E_{rms} = \sqrt{k_B T^2 C}$;
- $\Delta T(t) = \frac{\Delta E}{C} e^{-t/\tau}$ with $\tau = \frac{C}{G}$ and G thermal conductance.

HOLMES

Isotope candidate: ^{187}Re β decay $\Rightarrow$ $^{187}Re \rightarrow {}^{187}Os + e^- + \overline{\nu}_e$

Rhenium is perfectly suited for fabricating thermal detectors.

- Dielectric or superconductor behaviour;
- Very low end point: $Q = 2.47$ keV;
- Half-life time: $\tau_{1/2} = 43.2$ Gy;
- High natural abundance: $a.i. = 63\%$;
- Rate of 1 mg metallic Rhenium: $\simeq 1.0$ decay/s.

Metallic Rhenium single crystals

- Absorber: Re superconductor with $T_C = 1.6$ K;
- Sensor: NTD thermistors;
- MANU experiment (Genova).

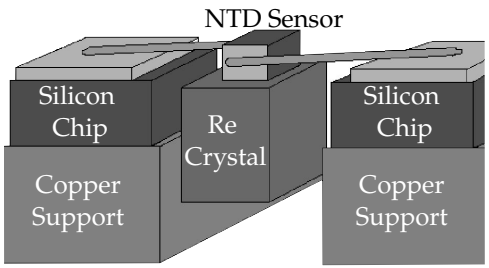

Dielectric Rhenium compound ($AgReO_4$) crystals

- Absorber: $AgReO_4$ crystals (Silver perrhenate);
- Sensor: Silicon implanted thermistors;
- MIBETA experiment (Milano, Como, Trento).

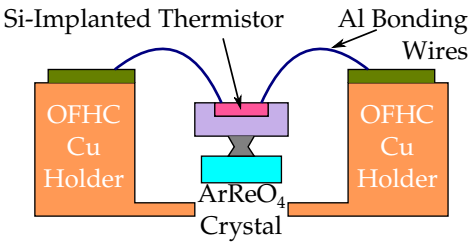

Calorimeters: present results

HOLMES

MANU (1999)

- 1 crystal of metallic Re: 1.6 mg;
- ^{187}Re activity: $\simeq$ 1.6 Hz;
- Sensor: Ge NTD thermistor:
- Resolution: $\Delta E = 96$ eV FWHM;
- Live-time: 0.5 years;
- $6.0 \cdot 10^6$ ^{187}Re decays above 420 eV.

$$m_\nu^2 = -462 \pm 579_{(stat)} \pm 679_{(sys)}\ eV^2$$

$$\Downarrow$$

$$m_\nu < 26\ eV\ (95\%\ C.L.)\ [14]$$

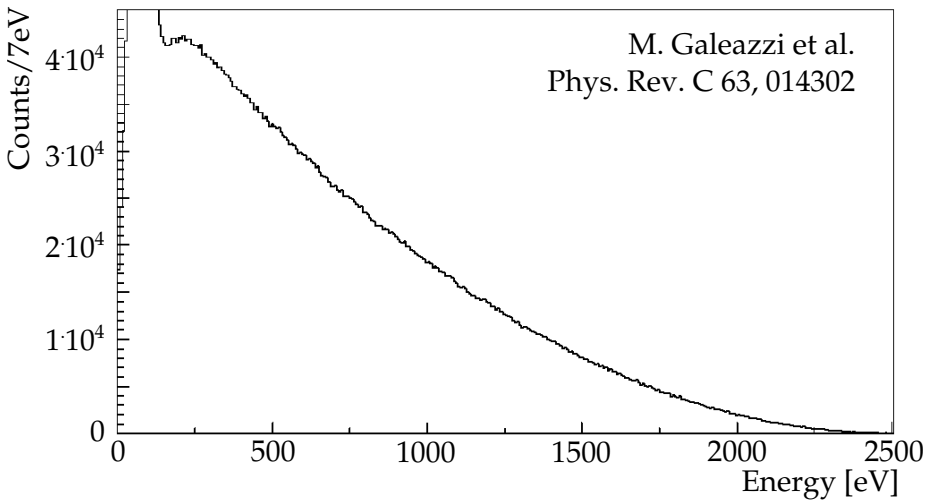

MIBETA (2002-2003)

- 10 $AgReO_4$ crystals: 2.71 mg;
- ^{187}Re activity: 0.54 Hz/mg;
- Sensor: Si thermistor (ITC-irst now FBK);
- Resolution: $\Delta E = 28.5$ eV FWHM;
- Live-time: 0.6 years;
- $6.2 \cdot 10^6$ ^{187}Re decays above 700 eV.

$$m_\nu^2 = -112 \pm 207_{(stat)} \pm 90_{(sys)}\ eV^2$$

$$\Downarrow$$

$$m_\nu < 15\ eV\ (90\%\ C.L.)\ [15]$$

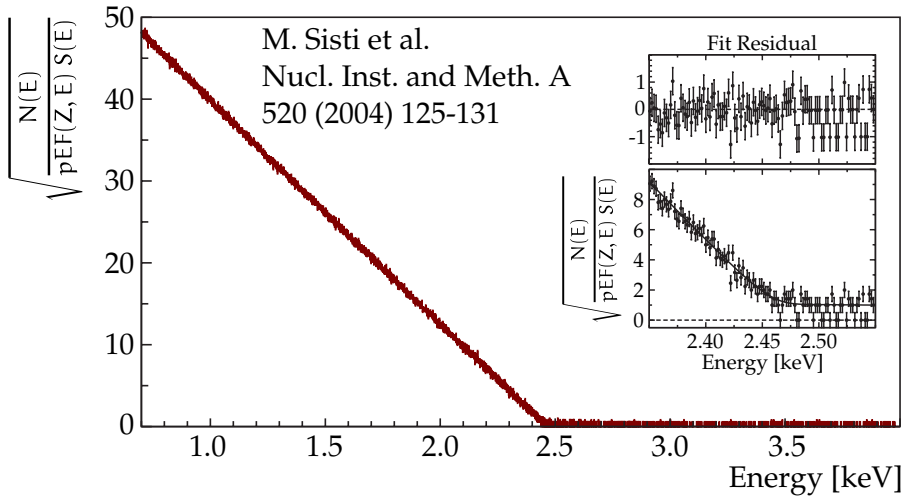

^{187}Re: improving m_ν sensitivity

Exposure required for $m_\nu = 0.2$ eV sensitivity [16]

A_β [Hz]	τ_{rise} [μs]	ΔE [eV]	N_{ev} [counts]	Exposure [det·year]
1	1	1	$0.2 \cdot 10^{14}$	$7.6 \cdot 10^5$
10	1	1	$0.7 \cdot 10^{14}$	$2.1 \cdot 10^5$
10	3	3	$1.3 \cdot 10^{14}$	$4.1 \cdot 10^5$
10	5	5	$1.9 \cdot 10^{14}$	$6.1 \cdot 10^5$
10	10	10	$3.3 \cdot 10^{14}$	$10.5 \cdot 10^5$

Example: *red line in table (background* $b = 0$*)*

- 5000 pixels/array;
- 8 arrays;
- 10 years of live-time;
- 400 g ^{nat}Re.

Exposure required for $m_\nu = 0.1$ eV sensitivity [16]

A_β [Hz]	τ_{rise} [μs]	ΔE [eV]	N_{ev} [counts]	Exposure [det·year]
1	0.1	0.1	$1.7 \cdot 10^{14}$	$5.4 \cdot 10^6$
10	0.1	0.1	$5.3 \cdot 10^{14}$	$1.7 \cdot 10^6$
10	1	1	$10.3 \cdot 10^{14}$	$3.3 \cdot 10^6$
10	3	3	$21.4 \cdot 10^{14}$	$6.8 \cdot 10^6$
10	5	5	$43.6 \cdot 10^{14}$	$13.9 \cdot 10^6$

Example: *green line in table (background* $b = 0$*)*

- 20000 pixels/array;
- 16 arrays;
- 10 years of live-time;
- 3.2 kg ^{nat}Re.

MARE: $AgReO_4$ with Si-implanted thermistors

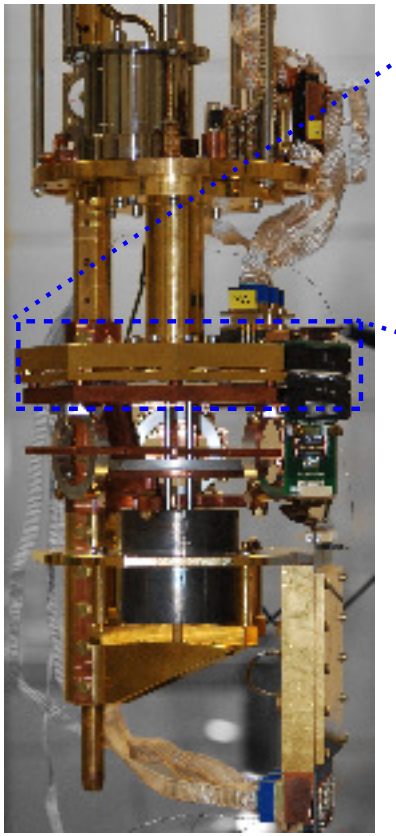

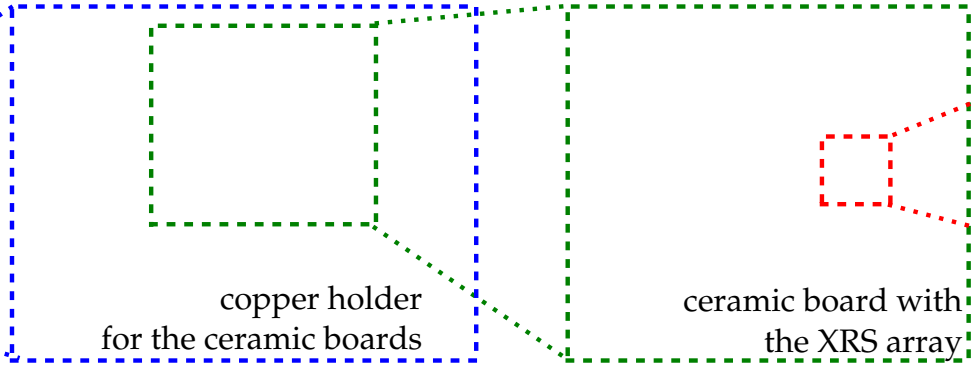

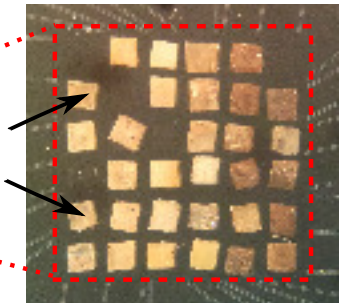

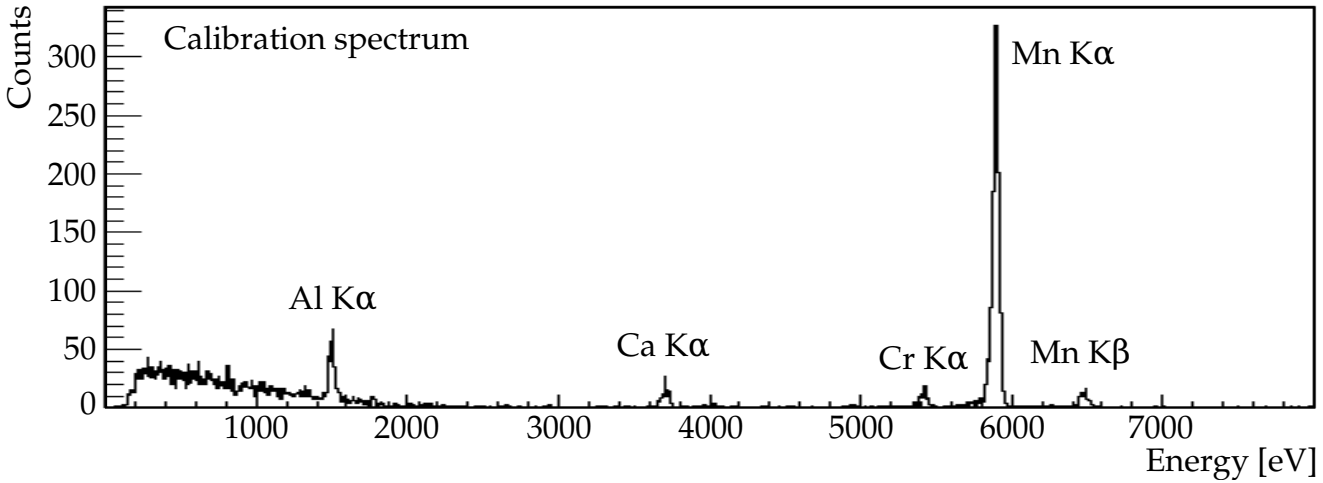

- 31 $AgReO_4$ crystals glued on 1st array;
- Only 16 usable: $\Delta E \simeq 47$ eV @ 2.6 keV, $\tau_{rise} \simeq 1$ ms;
- Not enough for improving previous m_ν limits
  $\Rightarrow$ $m_\nu \leqslant 10$ eV in 1 year of live time.

Status of Re detector development in about 20 years of test:

- To date no satisfactory results with Si- or Ge-thermistors but also with TES, MMCs;
- No clear understanding of Re absorber physics;
- Purity and superconductivity?
- Extra thermal capacity C due to nuclear quadrupole moment?
- low specific activity $\Rightarrow$ need large mass to reach sub-eV sensitivity;
- systematics due to the Beta Environmental Fine Structure (BEFS);
- ... and due to the detector response function.

$AgReO_4$ best detectors cannot provide the performances for sub-eV sensitivity

$\Downarrow$

with the current technologies the future of Re experiments is not very bright

The electron capture of the ^{163}Ho

An interesting isotope suitable for the neutrino mass experiment could be the ^{163}Ho.

$$^{163}Ho + e^- \rightarrow {}^{163}Dy^* + \nu_e(E_c) \quad \text{electron capture from shell} > M1$$

proposed by A. De Rujula e M. Lusignoli in 1982 [17, 18]

- Calorimetric measurement of Dy atomic de-excitations (mostly non-radiative):
  - $\Rightarrow$ measurement of the entire energy released except the ν energy;
- The rate at end-point may be as high as for ^{187}Re but depends on Q_{EC}:
- Q_{EC} and atomic de-excitation spectrum poorly known:
  - $\Rightarrow$ Measured: $Q_{EC} = (2.2 \div 2.8)$ keV;
  - $\Rightarrow$ Recommended: $Q_{EC} = 2.555$ keV [19, 20]);
- $\tau_{1/2} \simeq 4570$ years $\Rightarrow$ high specific activity:
  - $\Rightarrow$ Holmium detector not needed;
  - $\Rightarrow$ ^{163}Ho can be implanted in any suitable microcalorimeter absorber;
- Complex pile-up spectrum;
- No high statistics and clean calorimetric measurement so far;

^{163}Ho: EC spectrum

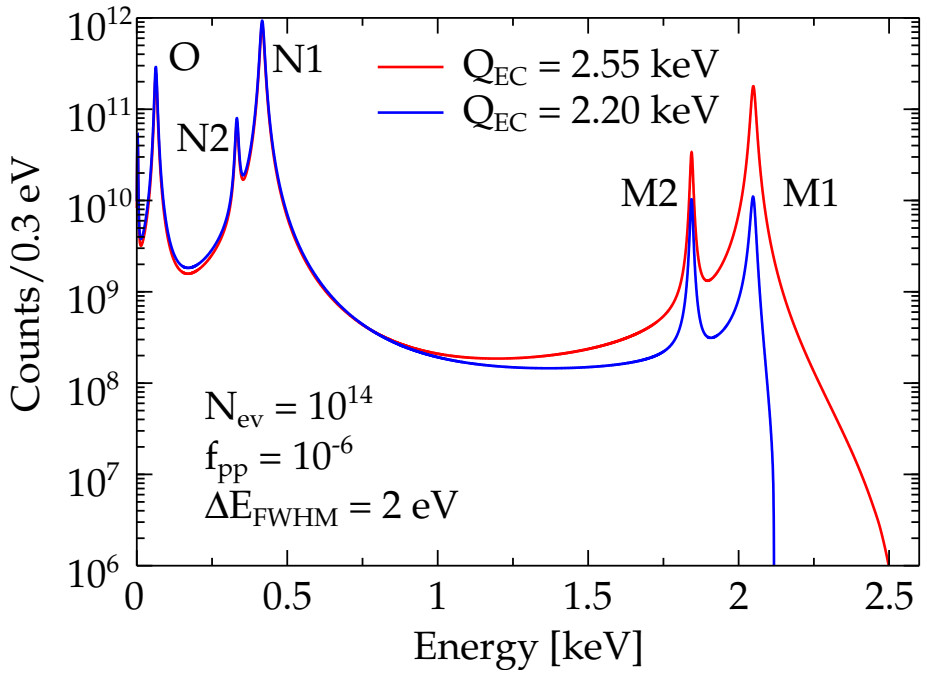

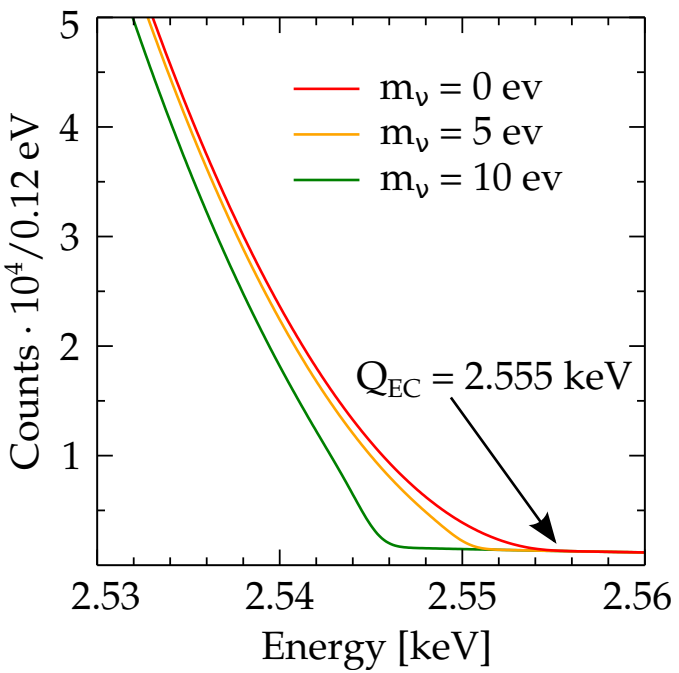

$$\frac{d\lambda_{EC}}{dE_c} = \frac{G_\beta^2}{4\pi^2}(Q_{EC}-E_c)\sqrt{(Q_{EC}-E_c)^2-m_\nu^2} \times \sum_i n_i C_i \beta_i^2 B_i \frac{\Gamma_i}{2\pi}\frac{1}{(E_c-E_i)^2+\Gamma_i^2/4},$$

- Continuum with marked peaks with Breit-Wigner shapes lines (width Γ_i of a few eV);
- Series of lines at the ionization energies E_i of the captured electrons;
- End-point shaped by $\sqrt{(Q-E_e)^2-m_\nu^2}$ (the same of the β-decay);
- Self calibrating spectrum;

^{163}Ho: pile-up spectra

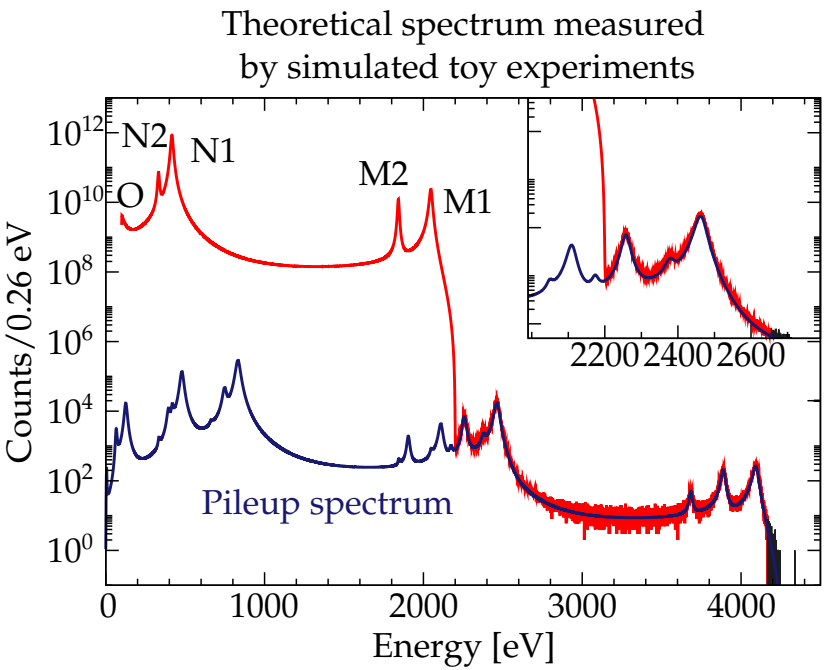

$$S(E_c) = \left[N_{ev}(N_{EC}(E_c, m_\nu) + f_{pp} \times N_{EC}(E_c, 0) \otimes N_{EC}(E_c, 0)) + B(E_c)\right] \otimes R_{\Delta E}(E_c)$$

$N_{EC}(E_c, m_\nu)$: ^{163}Ho spectrum
$B(E)$: background energy spectrum
$R_{\Delta E}(E_c)$: detector energy response function

more details in A. Nucciotti, submitted to EPJC, arXiv:1405.5060 [21]

- Pulse pile-up occurs when multiple events arrive within the temporal resolving time of the detector;
- Unresolved pile-up produces a sort of background close to the end-point;
- The ^{163}Ho pile-up events spectrum is quite complex and presents a number of peaks right at the end-point of the decay spectrum;
- To resolve pile-up:
  - Detector with fast signal rise-time τ_{rise};
  - Pulse pile-up recovery algorithm

^{163}Ho: statistical sensitivity

Montecarlo Simulation

- ^{163}Ho production: neutron irradiation of Erbium (Er) enriched ^{162}Er;
- ^{163}Ho embedded in thermal detectors for low energy X-rays spectroscopy;
- Rate: $2 \cdot 10^{11}$ nuclei of ^{163}Ho $\Rightarrow$ 1 decay/s;

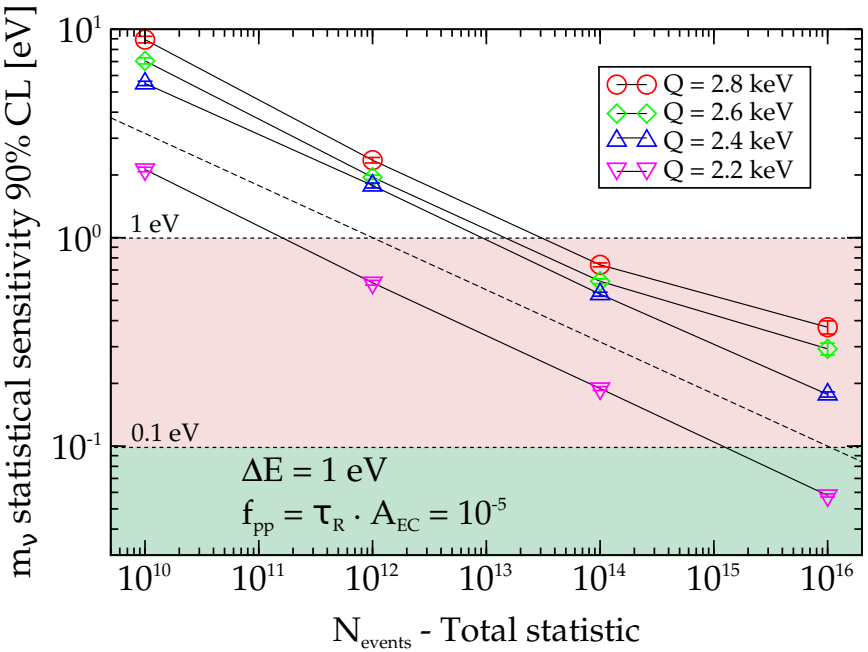

A. Nucciotti, submitted to EPJC, arXiv:1405.5060 [21]

Requirements:

- High energy resolution ($\simeq$ 1 eV);
- Fast response detectors ($\simeq$ 1 μs) to avoid pile-up events;
- Multiplexable detectors array ($\simeq$ 1000);

$\Downarrow$

TESs, MMCs, MKIDs, ...

^{163}Ho: experiment sensitivity for $Q_{EC} = 2200$ eV

Exposure required for $m_\nu = 0.2$ eV sensitivity [21, 22]

A_β [Hz]	τ_{rise} [μs]	ΔE [eV]	N_{ev} [counts]	Exposure [det·year]
1	1	1	$2.8 \cdot 10^{13}$	$9.0 \cdot 10^{5}$
1	0.1	1	$1.3 \cdot 10^{13}$	$4.3 \cdot 10^{5}$
100	0.1	1	$4.6 \cdot 10^{13}$	$1.5 \cdot 10^{4}$
10	0.1	1	$2.8 \cdot 10^{13}$	$9.0 \cdot 10^{4}$
10	1	1	$4.6 \cdot 10^{13}$	$1.5 \cdot 10^{5}$

Example: *green line in table (background* $b = 0$*)*

- 5000 pixels/array;
- 3 arrays;
- 1 years of live-time;
- $2 \cdot 10^{17}$ nuclei of ^{163}Ho

Exposure required for $m_\nu = 0.1$ eV sensitivity [21, 22]

A_β [Hz]	τ_{rise} [μs]	ΔE [eV]	N_{ev} [counts]	Exposure [det·year]
1	0.1	0.3	$1.2 \cdot 10^{14}$	$3.9 \cdot 10^{6}$
100	0.1	0.3	$6.4 \cdot 10^{14}$	$2.0 \cdot 10^{5}$
100	0.1	1	$7.4 \cdot 10^{14}$	$2.4 \cdot 10^{5}$
10	0.1	1	$4.5 \cdot 10^{14}$	$1.5 \cdot 10^{6}$
10	1	1	$7.4 \cdot 10^{14}$	$2.4 \cdot 10^{6}$

Example: *red line in table (background* $b = 0$*)*

- 5000 pixels/array;
- 4 arrays;
- 10 years of live-time;
- $3 \cdot 10^{17}$ nuclei of ^{163}Ho

^{163}Ho: experiment sensitivity for $Q_{EC} = 2800$ eV

Exposure required for $m_\nu = 0.2$ eV sensitivity [21, 22]

A_β [Hz]	τ_{rise} [μs]	ΔE [eV]	N_{ev} [counts]	Exposure [det·year]
1	1	1	$0.2 \cdot 10^{14}$	$7.6 \cdot 10^{5}$
1	0.1	1	$1.6 \cdot 10^{15}$	$5.3 \cdot 10^{7}$
100	0.1	1	$9.8 \cdot 10^{15}$	$3.1 \cdot 10^{6}$
10	0.1	1	$3.8 \cdot 10^{15}$	$1.2 \cdot 10^{7}$
10	1	1	$9.8 \cdot 10^{15}$	$3.1 \cdot 10^{7}$

Example: *green line in table (background* $b = 0$*)*

- 60000 pixels/array;
- 5 arrays;
- 5 years of live-time;
- $4 \cdot 10^{18}$ nuclei of ^{163}Ho

Exposure required for $m_\nu = 0.1$ eV sensitivity [21, 22]

A_β [Hz]	τ_{rise} [μs]	ΔE [eV]	N_{ev} [counts]	Exposure [det·year]
1	0.1	0.3	$2.6 \cdot 10^{16}$	$8.2 \cdot 10^{8}$
100	0.1	0.3	$1.9 \cdot 10^{17}$	$5.9 \cdot 10^{7}$
100	0.1	1	$1.6 \cdot 10^{17}$	$5.0 \cdot 10^{7}$
10	0.1	1	$6.1 \cdot 10^{16}$	$1.9 \cdot 10^{8}$
10	1	1	$1.6 \cdot 10^{17}$	$5.0 \cdot 10^{8}$

Example: *red line in table (bkg=0*

- 10^6 pixels/array;
- 6 arrays;
- 10 years of live-time;
- $8 \cdot 10^{19}$ nuclei of ^{163}Ho

Holmium LTD experiment status

^{163}Ho seems to be better than ^{187}Re:

- ☺ higher specific activity ⇒ Holmium detector not needed;
- ☺ self calibrating ⇒ better systematics control;
- ☹ Q_{EC} and atomic de-excitation spectrum poorly known;
- ☹ complex pile-up spectrum;
- ☹ in case of higher Q ⇒ less sensitive;

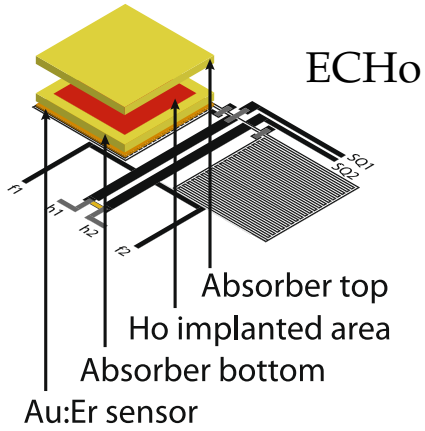

(At least) two LTD projects with ^{163}Ho:

- ECHo, MMC detectors (Heidelberg)
- HOLMES, TES detectors (Milano, Genova, LNGS, NIST)
- Los Alamos Nat. Lab., Berkeley Univ., ...

Common technical challenges:

- Clean ^{163}Ho production;
- ^{163}Ho incorporation;
- Large channel number ⇒ high speed MUX;
- Data handling (processing, storage, ...)

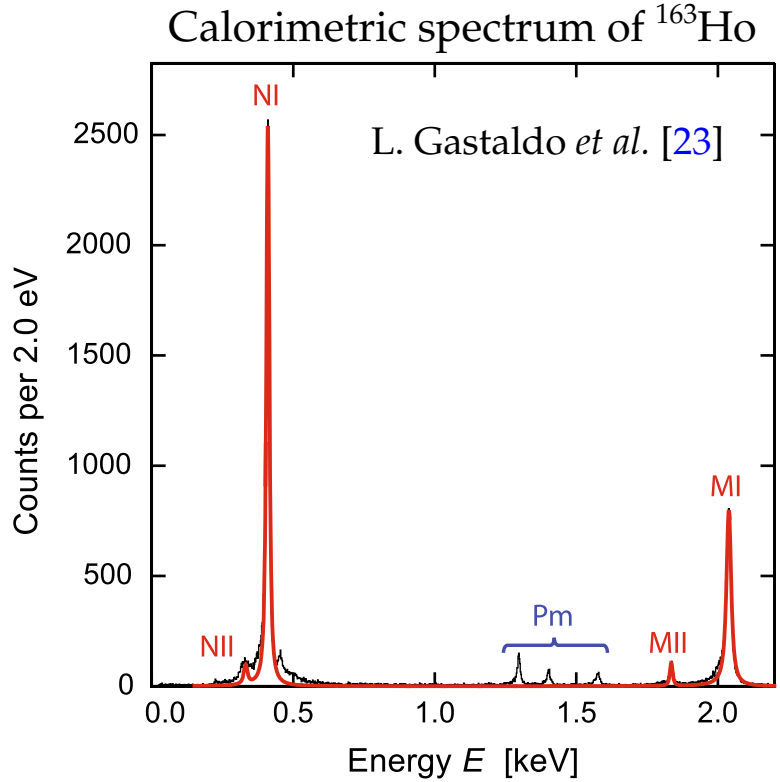

HOLMES (ERC-Advanced Grant n. 340321)

Goal

- Neutrino mass measurement:
  $\Rightarrow$ m_ν statistical sensitivity as low as 0.4 eV;
- Prove technique potential and its scalability (Megapixel experiment);
- assess EC Q-value;
- assess systematic errors;

Baseline

- Transition Edge Sensors (TES) with ^{163}Ho implanted Bi:Au absorbers;
- $6.5 \cdot 10^{13}$ nuclei per detector $\Rightarrow$ 300 dec/s;
- $\Delta E \simeq 1$ eV and $\tau_{rise} \simeq 1$ µs;
- 16 channel demonstrator/1000 channel final array;
- $3 \cdot 10^{13}$ events in 3 years;

Project Start: 1 Feb 2014

http://artico.mib.infn.it/nucriomib/experiments/holmes

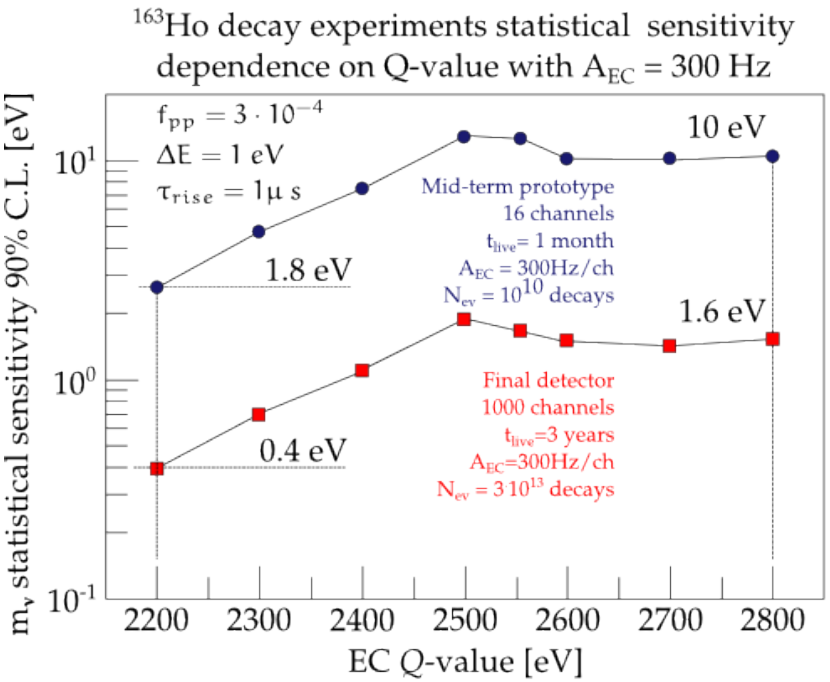

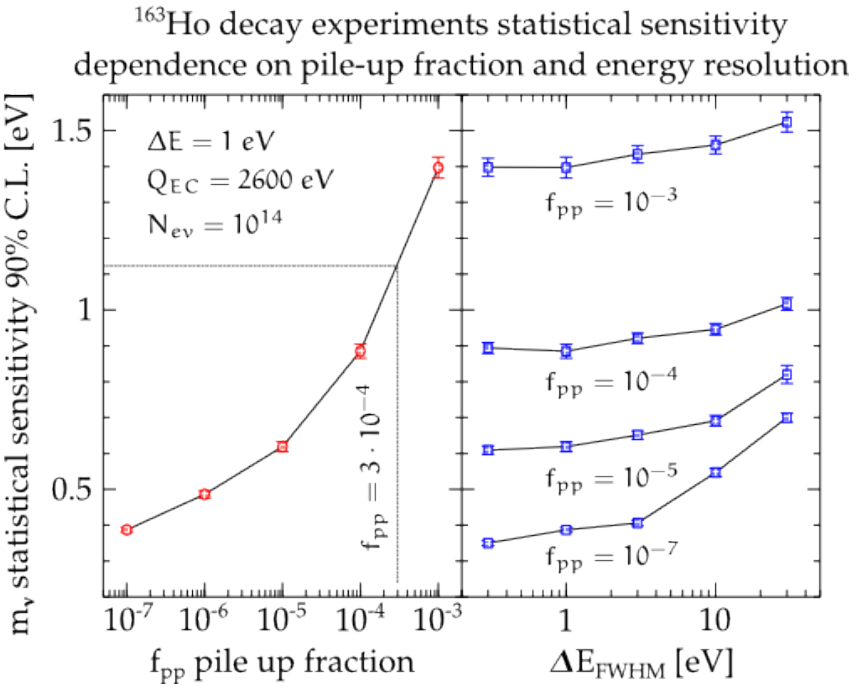

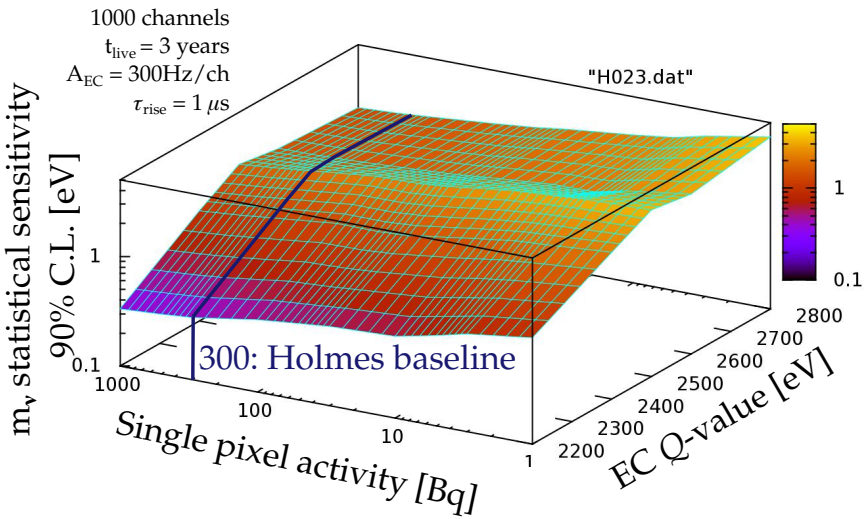

- The experimental sensitivity is directly related to $f_{pp} = \tau_{rise} \cdot A_{EC}$ (pile-up);
- The impact of the energy resolution is relatively smaller than that of pile-up;
- In presence of a high level of pile-up, the experiment is relatively less sensitive to the energy resolution;

Effect of background on sensitivity

Background sources:

- Environmental γ radiation:
  - Compton interactions;
  - Photoelectric interactions with photoelectron escape;
  - Fluorescent X-rays and X-ray escape lines;
- γ and β from close surroundings;
- Cosmic rays at sea level (muons):
  - Au pixel: $200 \times 200 \times 3\ \mu m^3$
    $\Rightarrow\ E \simeq 10\ keV, rate \simeq 1\ d^{-1}$;
  - Si chip: $20 \times 20 \times 0.5\ mm^3$
    $\Rightarrow\ E \simeq 300\ keV, rate \simeq 7000\ d^{-1}$;

Experimental results:

- MIBETA: $300 \times 300 \times 150\ \mu m^3$ $AgReO_4$ crystals:
  $\Rightarrow\ b(2..5keV) \simeq 1.5 \cdot 10^{-4}$ c/eV/d/det;
- TES @NIST (1600m): $350 \times 350 \times 2.5\ \mu m^3$ Bi absorbers:
  $\Rightarrow\ b < 1$ c/eV/d/det (preliminary);

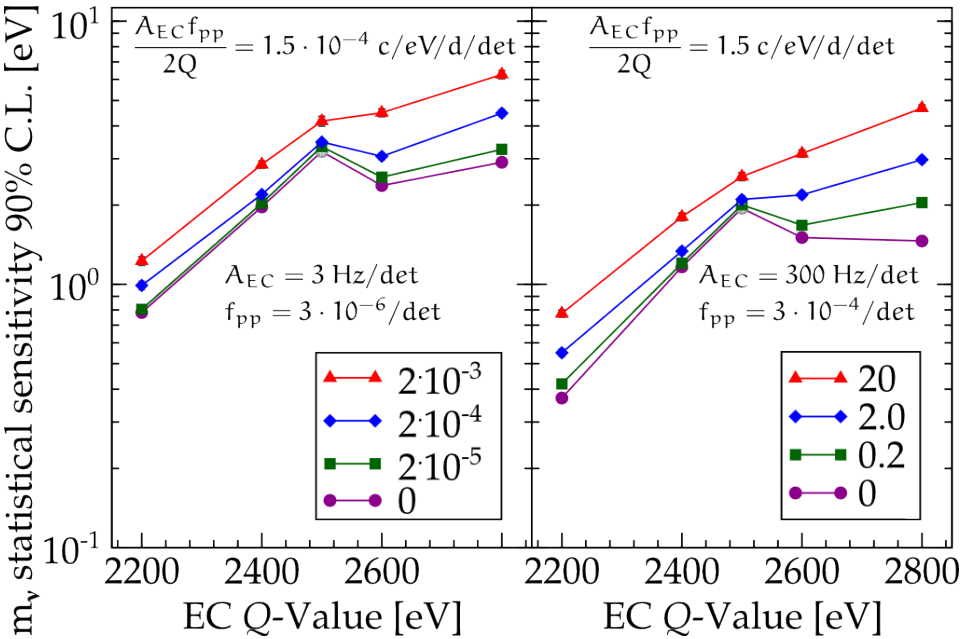

$\Downarrow$

A constant background b is negligible if it is much smaller than the pile-up spectrum

$$b << \frac{A_{EC} \cdot f_{pp}}{2Q_{EC}}$$

For large activities A_{EC}, and correspondingly large pile-up rate, the statistical sensitivity should be relatively insensitive to cosmic rays and to environmental radioactivity.

HOLMES Tasks

- ^{163}Ho isotope production;
- ^{163}Ho isotope embedding in detector;
- Single TES optimization and testing;
- TES array design, engineering and testing;
- SQUID read-out and multiplexing optimization and testing (rf-SQUID);
- Real time and offline signal processing and analysis (trigger, OF filter, pile-up rejection);
- Cryogenic set-up (new LHe-free cryostat, pulse-tube assisted);

Development in two steps:

- First demonstrator prototype: 16 pixel prototype;
- Final detector array: 1000 pixel;

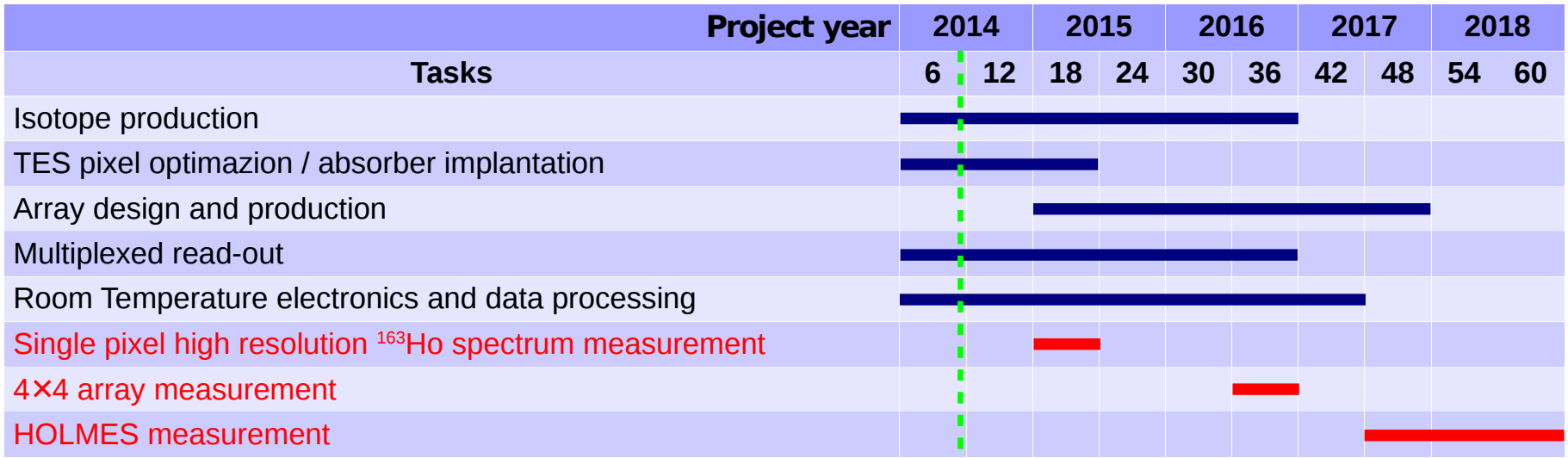

^{163}Ho production

Neutron reactor activation:

Enriched ^{162}Er targets for indirect production of ^{163}Ho

$$^{162}\mathrm{Er}(n,\gamma)^{163}\mathrm{Er} \rightarrow {}^{163}\mathrm{Ho} + \nu_e \quad , \quad \sigma_{therm} = 20\mathrm{b} \quad , \quad \tau_{EC}^{1/2} = 75\ \mathrm{min}$$

- Requires ^{162}Er enrichment (nat i.a.=0.139%) and oxide chemical form (Er_2O_3);
- $3 \cdot 10^{12}$ ^{163}Ho nuclei/mg(^{162}Er)/h for a thermal flux of 10^{13} n/cm^2/s;
- Not all cross sections are known: the process will be studied;
- Unavoidable ^{166m}Ho: $^{165}\mathrm{Ho}(n,\gamma)^{166m}\mathrm{Ho}$ (β, $_{12} = 1200$ y) from Ho contaminations or ^{164}Er(n,γ);
- Unavoidable ^{164}Ho: fast neutron activation $^{163}\mathrm{Ho}(n,\gamma)^{164}\mathrm{Ho}$

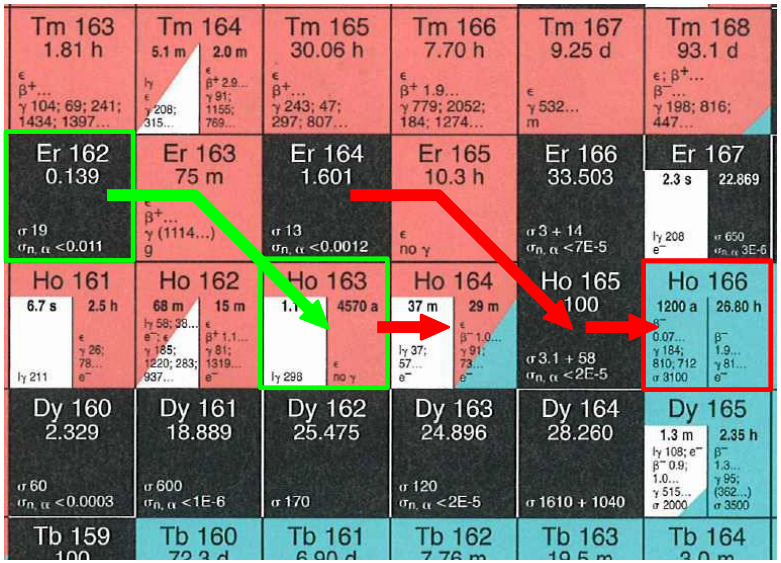

Thermoreduction to obtain the metallic Ho target for implantation:

$$\mathrm{Ho_2O_3} + 2\mathrm{Y(met)} \rightarrow$$
$$2\mathrm{Ho(met)} + \mathrm{Y_2O_3} \ @\ 2000^\circ\mathrm{C}$$

^{163}Ho embedding

Implant procedure:

- magnetic mass separation to separate ^{163}Ho from Dy, Er and more;
- ^{163}Ho embedding in the detector absorber;

Ion implanter:

- Ionic source: Penning sputter source with metallic ^{163}Ho/Er/Au anode;
- Mass-analysis magnet for ion beam extracted from the ion source;
- Acceleration mechanics: ions electrostatically accelerated to a high energy;
- Target chamber: ions (^{163}Ho) impinge on a target (TES absorber, Au);
- $20 \div 30$ KeV for $50 \div 100$ nm penetration in Au;

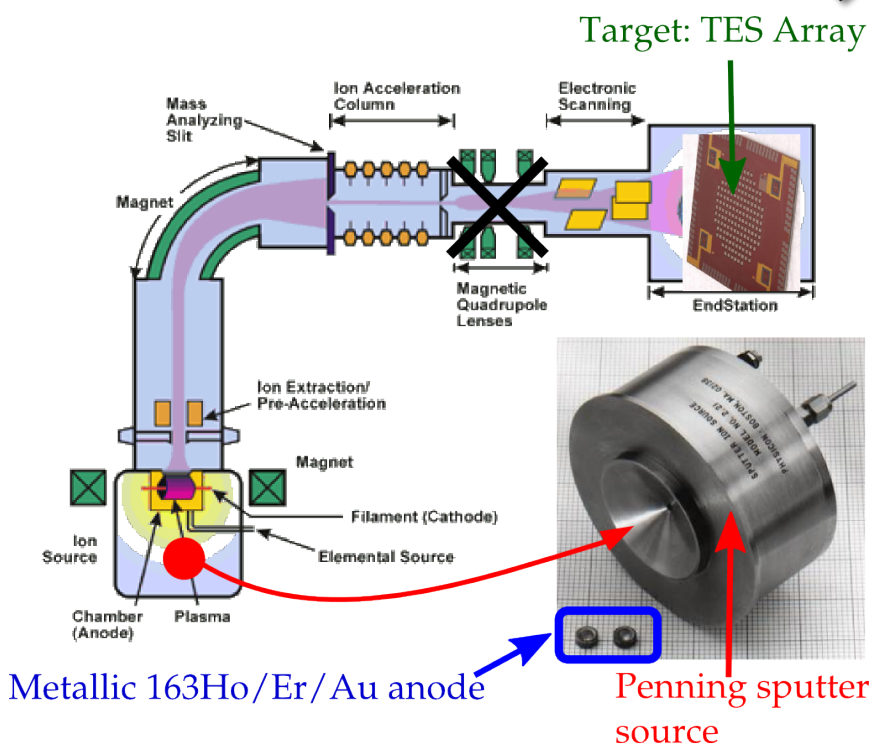

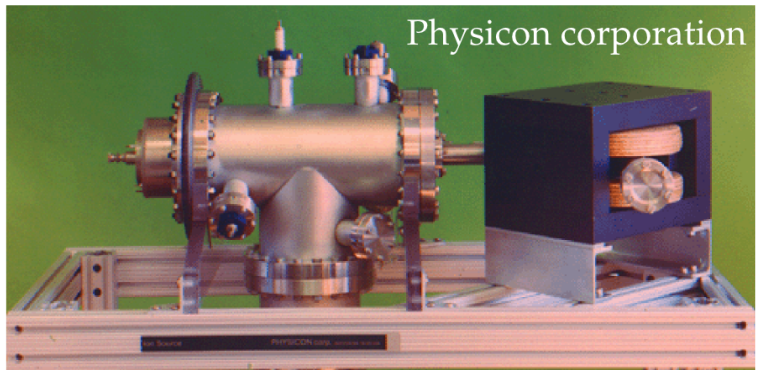

Transition Edge Sensor (TES): cryogenic particle detector that exploits the strongly temperature-dependent resistance of the superconducting phase transition.

- Superconductor biased in its transition;
- "Self-biased region" $\Rightarrow$ the power dissipated in the device is constant with the applied bias;
- Electrothermal feedback: if $R_{TES} \uparrow \Rightarrow I_{TES} \downarrow \Rightarrow P_J \downarrow \Rightarrow$ cooling the device back to its equilibrium state in the self-biased region;
- Low resistance: read out with SQUIDs (Superconducting Quantum Interference Devices);
- TES operates in series with the input coil L which is inductively coupled to a SQUID series-array:
- Change in TES current $\Rightarrow$ change in the input flux to the SQUID;
- The SQUID output is further amplified and read by room-temperature electronics;

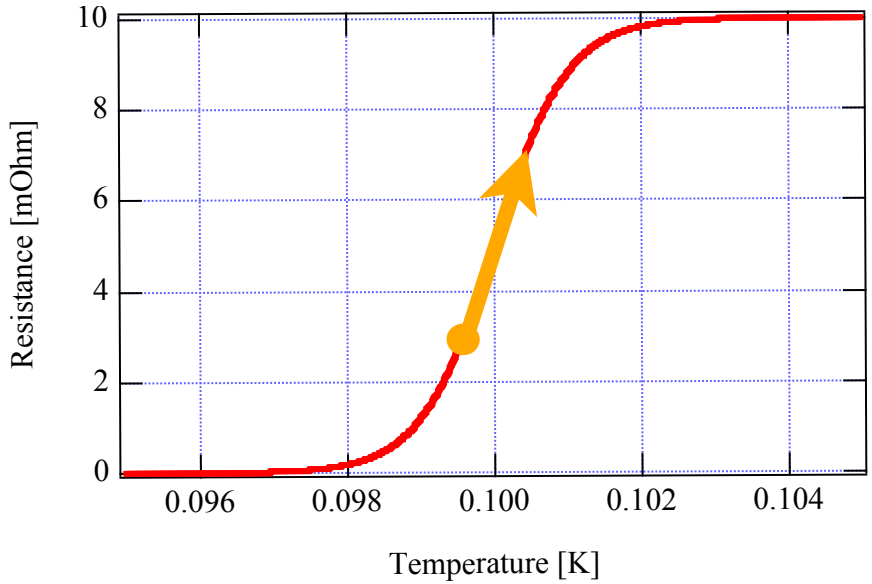

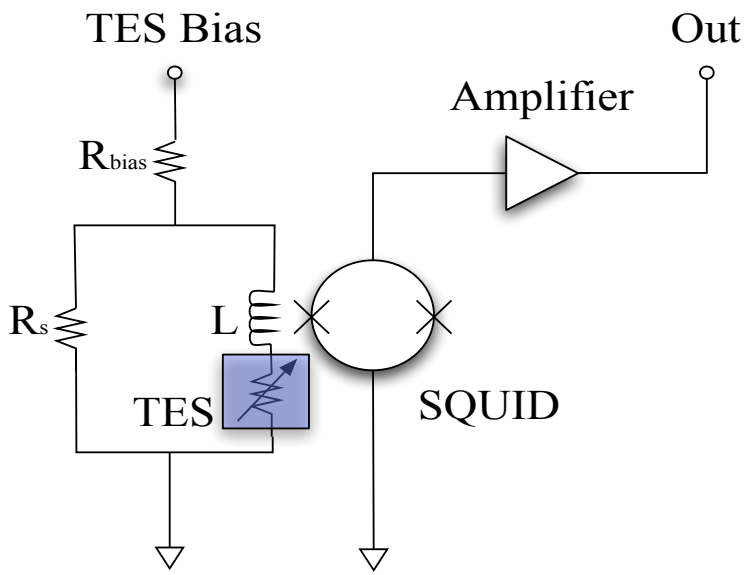

Why TES?

- Strongly supported by the X-ray astrophysics community for the past couple of decades (but also Dark Matter and rare events research);
- Small size $\Rightarrow$ low thermal capacity C $\Rightarrow$ excellent energy resolution:

$$\Delta E_{FWHM} = \begin{cases} 1.26eV \,@\, 1.5\ keV \\ 1.58eV \,@\, 6\ keV \\ 1.94eV \,@\, 8\ keV \end{cases}$$

- The negative electro-thermal feedback provides a fast time response;
- Large Array and multiplexing (TDM, CDM and FDM);
- Cross-talk between pixels less than 0.01%;
- Tunable critical temperature T_C exploiting the proximity effect [24] $\Rightarrow$ Mo:Au or Mo:Cu proximity TES ($T_C \simeq 100$ mK);

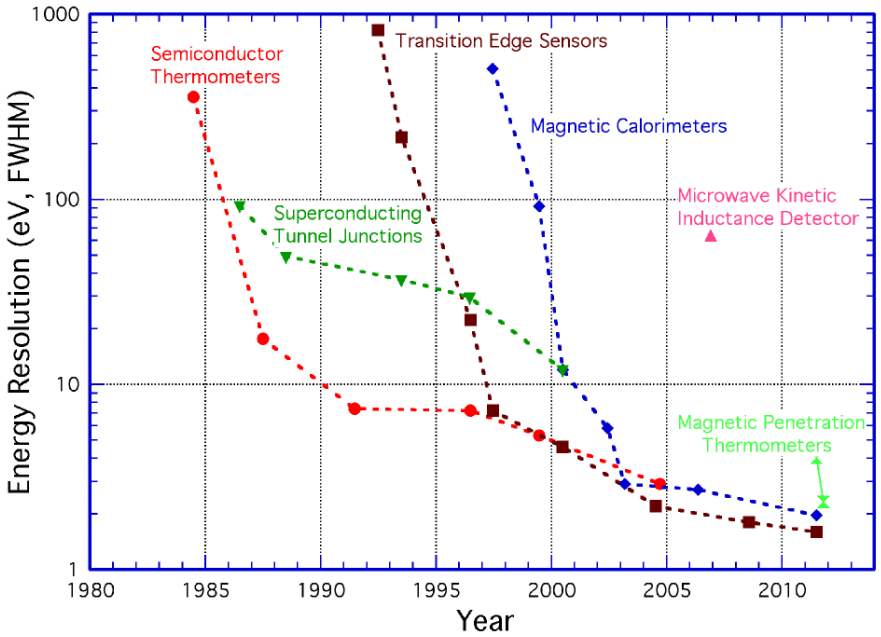

TESs are natural candidates to reach an energy resolution of 1 eV and a time resolution of 1 µs

TES Resolution

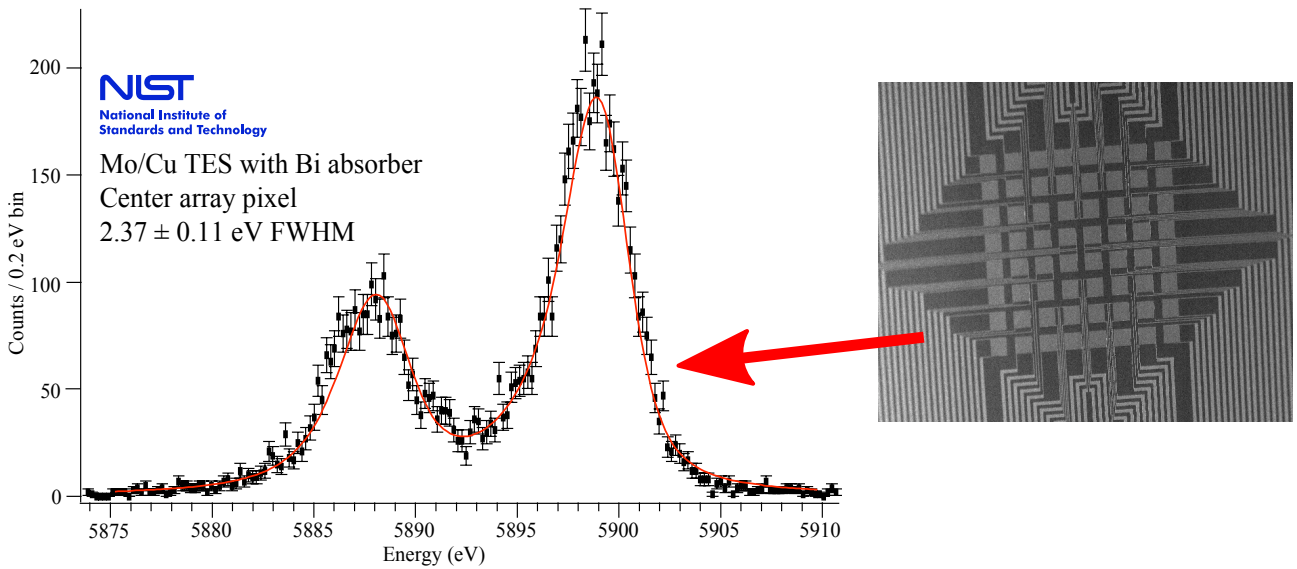

NASA/Goddard Space Flight Center

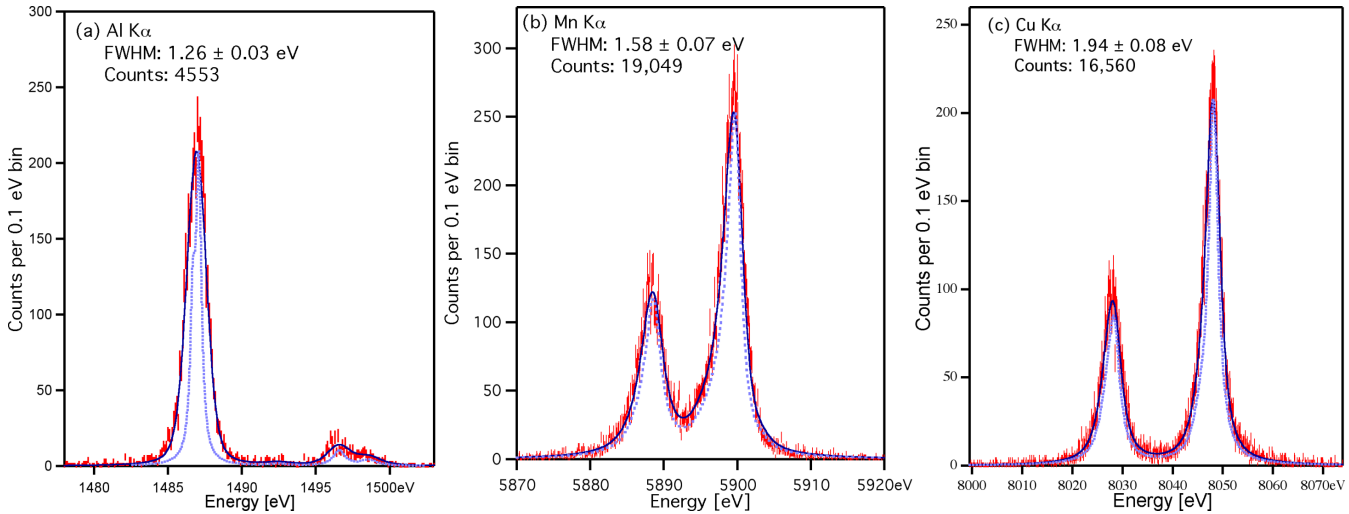

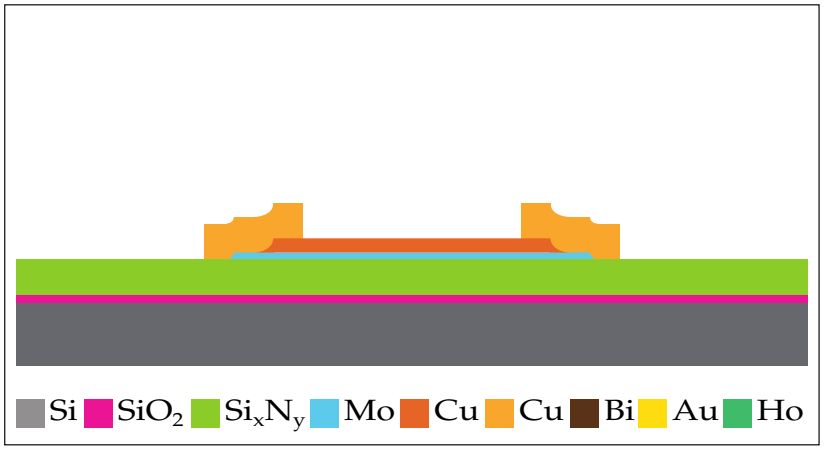

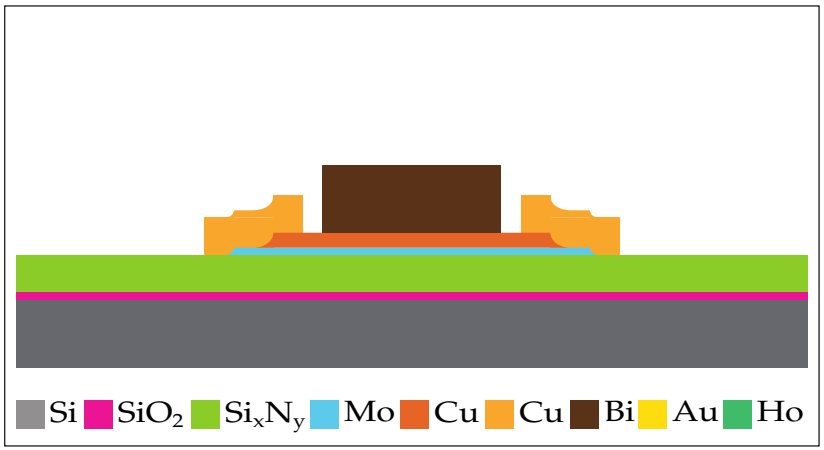

Phase 1 @NIST

- Mo:Cu proximity TES ($T_C \simeq 100$ mK) [24];
- SiO_2 stopper layer;
- Si_xN_y membrane for thermal insulation;
- deposited on a Si substrate.

Phase 2 @NIST

Bismuth deposition for the first absorber layer ($2 \div 4\mu$ m) by lift-off process:

- Photoresist deposition (sacrificial layer);
- Target material (Bi) deposition;
- Wash out of the sacrificial layer;

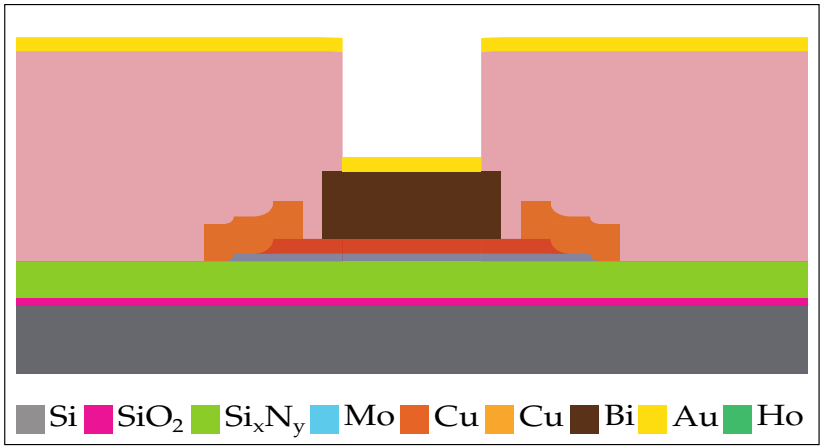

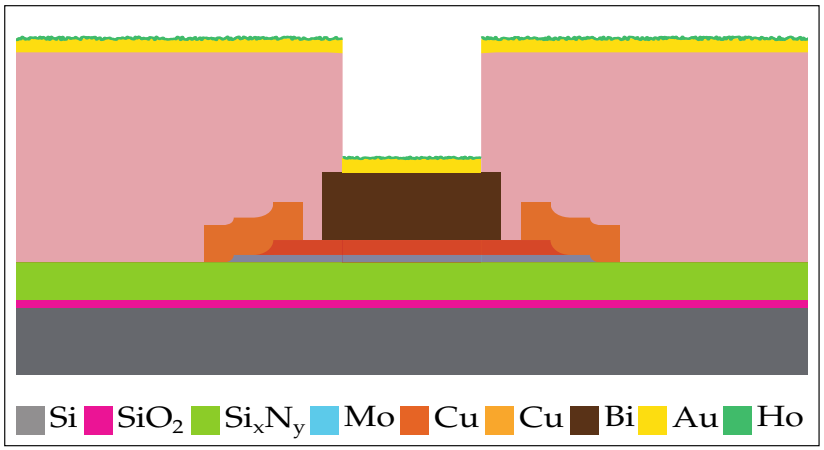

Phase 3 @NIST

Gold deposition for the second absorber layer ($0.1 \div 0.2$ µm):

- Lift-off not finished (no photoresit wash out);
- Ship to Genova (for the ^{163}Ho implant;

Phase 4 @Genova

^{163}Ho implanting:

- Metallic ^{163}Ho/Er/Au anode (source);
- Magnetic mass separation;
- Implantation and magnetic separation;

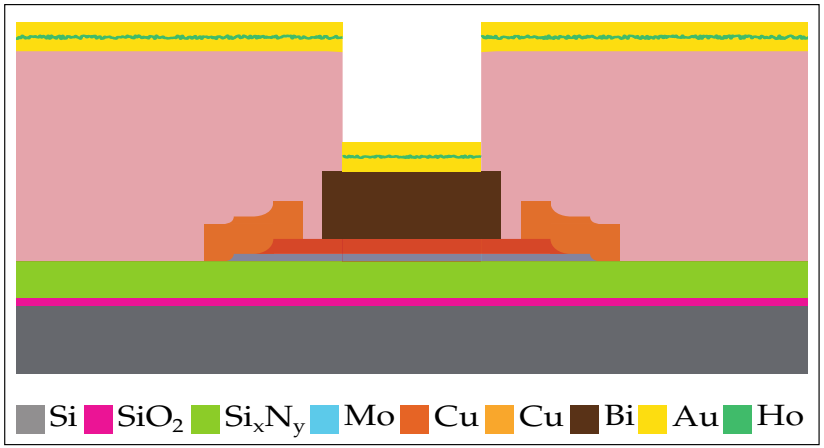

Phase 5 @Genova

Gold film deposition for full containment:

- ^{163}Ho coating with thin Au ($0.1 \div 0.2$ μm) layer;

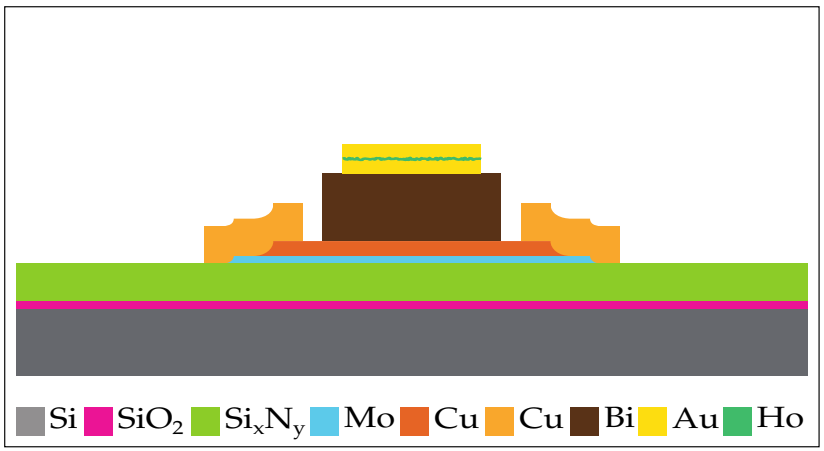

Phase 6 @Genova

Lift-off of the Au:Ho:Au layer:

- ^{163}Ho-implanted Au-absorber.

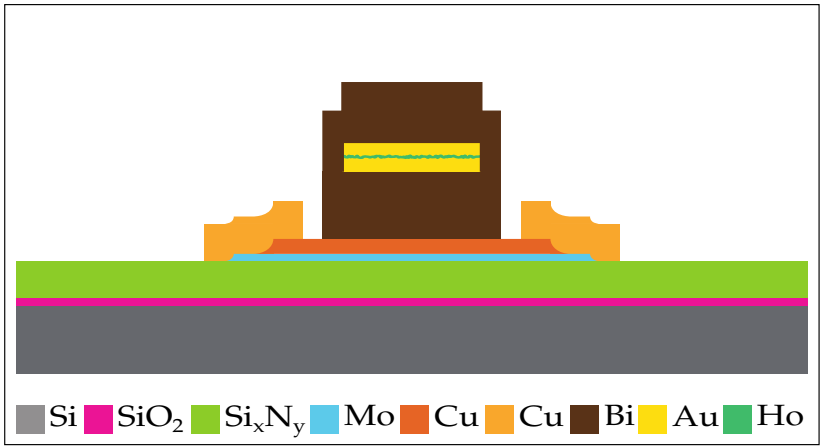

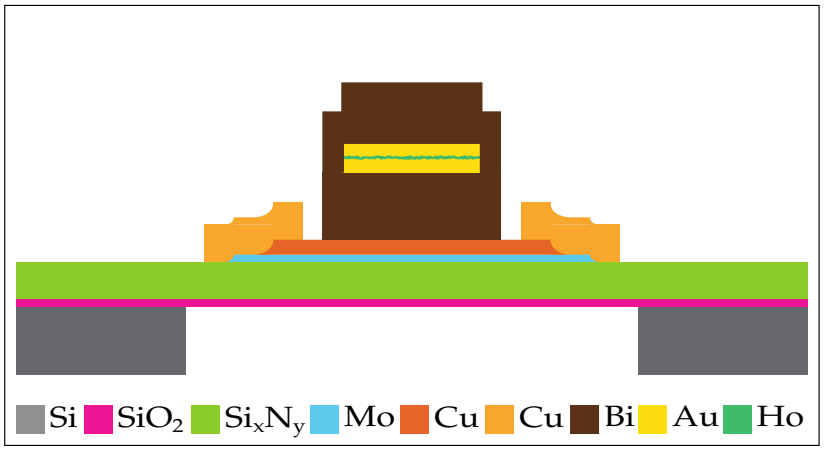

Phase 7 @Genova

Second Bi absorber layer ($2 \div 4$ μm):

- Bi fully encapsulates Au:Ho layer;

Phase 8 @Genova (final fabrication phase)

Deep reactive ion etching (DRIE) to remove Si substrate (and to achieve necessary thermal isolation):

- Suspended TES with Bi:Cu absorber ^{163}Ho-implanted (T-shaped);
- Ship to Milano;
- Installation in the Cryogenics facility;

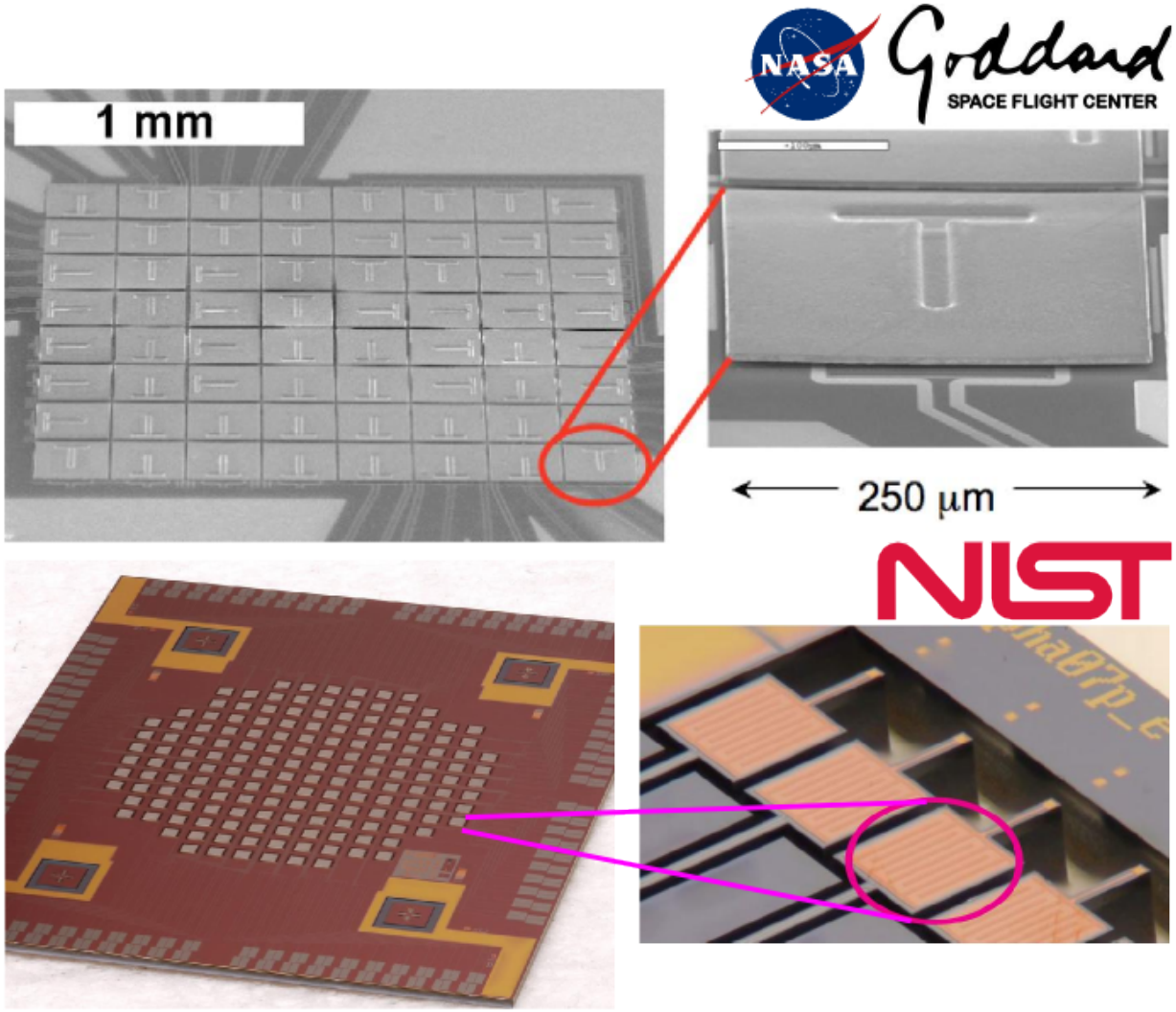

NIST design is the starting point for the HOLMES array detector: 4×256 pixel

The

rf-SQUID read-out

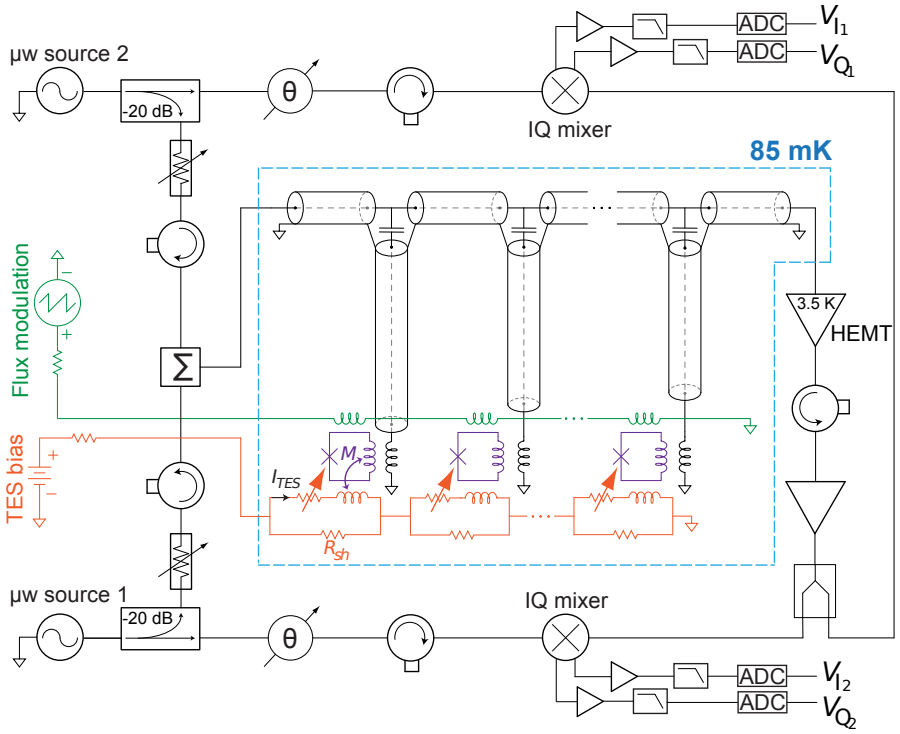

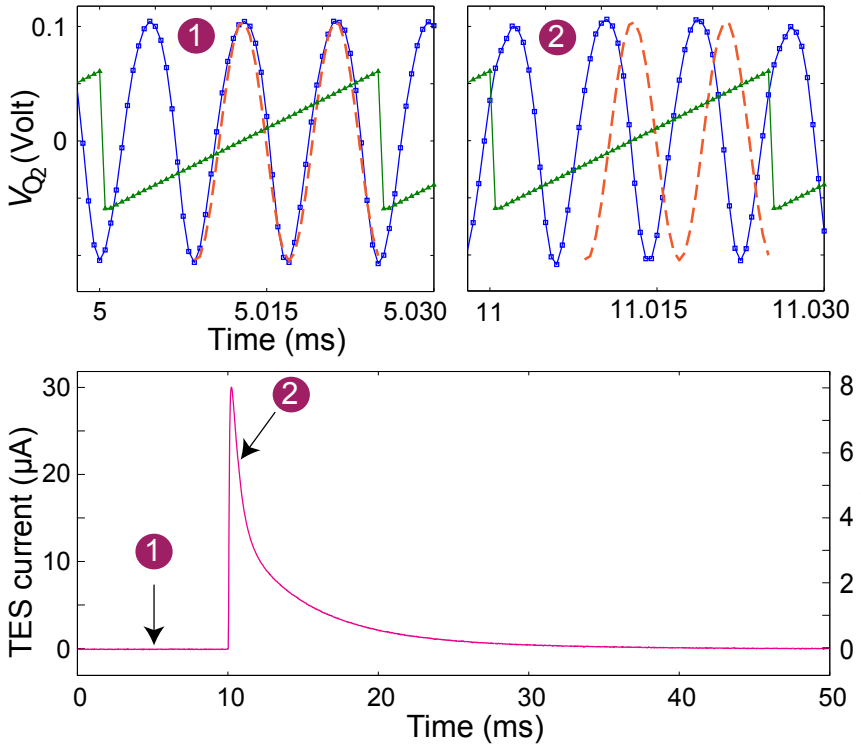

- DC biased TES (1 bias for all TESs);
- SQUID coupled with TES and a resonator circuit;
- Microwave rf-SQUID read out with flux ramp modulation (common flux line is inductively coupled to all the SQUIDs);
- Signal reconstructed by homodyne detection (IQ signal de-multiplexing) and demodulation;

- 2 Channels demonstrator @NIST [25];
- Bandwidth/pixel 10MHz $\Rightarrow$ 50 resonances between 0 and 500MHz (typical commercial ADC range);

ROACH2-based Multiplexing

- Reconfigurable Open Architecture Computing Hardware (ROACH) designed by the Collaboration For Astronomy Signal Processing and Electronics Research (CASPER);
- Xilinx Virtex FPGA based digital data processing;
- Frequency comb generation ($\simeq$ 60 tones in the $0 \div 550$ MHz range);
- Quadrature frequency upmixing (500 MHz $\rightarrow$ 5 GHz) and down-mixing (5 GHz $\rightarrow$ 500 MHz);
- Signal channelizing and rf-SQUID signal de-modulation
- Real time signal processing;
- Strongly tested for MKIDs read-out (ARCONS, 2048 pixels);

Design for HOLMES:

- $4 \times 256 = 1024$ pixels;
- Target: 64 resonace per ROACH-module;
- Complete system composed by 16 module.

Conclusion

- The measurement of the end point of nuclear beta or electron capture (EC) decays spectra is the only model-independent;
- The goal of the next generation experiments is the sub-eV neutrino mass sensitivity;
- The HOLMES experiment will performe a direct measurment of the nuetrino mass by using microcalorimenter with absorber ^{163}Ho-implanted;
- The Goals of the HOLMES experiment are:
  - assess EC Q-value of the ^{163}Ho;
  - assess systematic errors;
  - achieve a statistical sensitivity as low as 0.4 eV;
  - prove technique potential and its scalability (Megapixel experiment);

[1] F. Capozzi, G.L. Fogli, E. Lisi, A. Marrone, D. Montanino et al., **"Status of three-neutrino oscillation parameters, circa 2013"**, 2013, e-print: arXiv:1312.2878 [hep-ph].

[2] Stefano Dell'Oro, Simone Marcocci and Francesco Vissani, **"New expectations and uncertainties on Neutrinoless Double Beta Decay"**, 2014, e-print: arXiv:1404.2616 [hep-ph].

[3] Srubabati Goswami, Abhijit Bandyopadhyay and Sandhya Choubey, **"Global analysis of neutrino oscillation"**, *Nuclear Physics B - Proceedings Supplements*, vol. 143, no. 0, no. 0, pp. 121 – 128, 2005, doi:10.1016/j.nuclphysbps.2005.01.096.

[4] Mark Wyman, Douglas H. Rudd, R. Ali Vanderveld and Wayne Hu, **"$\nu\Lambda$CDM: Neutrinos help reconcile Planck with the Local Universe"**, *Phys.Rev.Lett.*, vol. 112, p. 051302, 2014, doi:10.1103/PhysRevLett.112.051302, e-print: arXiv:1307.7715 [astro-ph.CO].

[5] M. Agostini et al. (GERDA Collaboration), **"Results on Neutrinoless Double-β Decay of ^{76}Ge from Phase I of the GERDA Experiment"**, *Phys. Rev. Lett.*, vol. 111, no. 12, no. 12, p. 122503, 2013, doi:10.1103/PhysRevLett.111.122503, e-print: arXiv:1307.4720 [nucl-ex].

[6] J.B. Albert et al. (EXO-200 Collaboration Collaboration), **"Search for Majorana neutrinos with the first two years of EXO-200 data"**, 2014, e-print: arXiv:1402.6956 [nucl-ex].

[7] V.M Lobashev et al., **"Direct search for neutrino mass and anomaly in the tritium beta-spectrum: Status of troitsk neutrino mass experiment",** *Nucl. Phys. B. (Proc. Suppl.)*, vol. 91, no. 13, no. 13, pp. 280–286, 2001, doi:10.1016/S0920-5632(00)00952-X.

[8] Ch. Kraus et al., **"Final results from phase II of the Mainz neutrino mass searchin tritium β decay",** *Eur. Phys. J. C*, vol. 40, no. 4, no. 4, pp. 447–468, 2005, doi:10.1140/epjc/s2005-02139-7.

[9] Christine Kraus, Andrej Singer, Kathrin Valerius and Christian Weinheimer, **"Limit on sterile neutrino contribution from the Mainz Neutrino Mass Experiment",** *Eur. Phys. J. C*, vol. 73, p. 2323, 2013, doi:10.1140/epjc/s10052-013-2323-z, e-print: `arXiv:1210.4194 [hep-ex]`.

[10] A. Picard et al., **"A solenoid retarding spectrometer with high resolution and transmission for kev electrons",** *Nuclear Instruments and Methods in Physics Research Section B: Beam Interactions with Materials and Atoms*, vol. 63, no. 3, no. 3, pp. 345 – 358, 1992, doi:10.1016/0168-583X(92)95119-C.

[11] V.N. Aseev et al. (Troitsk Collaboration Collaboration), **"An upper limit on electron antineutrino mass from Troitsk experiment",** *Phys.Rev. D*, vol. 84, p. 112003, 2011, doi:10.1103/PhysRevD.84.112003, e-print: `arXiv:1108.5034 [hep-ex]`.

[12] J. Angrik et al., **"KATRIN design report 2004",** *Tech. Rep., Forschungszentrum, Karlsruhe, Germany*, pp. 447–468, 2004.
NPI ASCR Řež, EXP-01/2005, FZKA Scientific Report 7090, MS-KP-0501.

[13] Michael Sturm, **"Status of the KATRIN experiment with special emphasis on source-related issues"**, 2011, e-print: arXiv:1111.4773 [hep-ex].

[14] M. Galeazzi, F. Fontanelli, F. Gatti and S. Vitale, **"End-point energy and half-life of the 187re β decay"**, *Phys. Rev. C*, vol. 63, p. 014302, 2000, doi:10.1103/PhysRevC.63.014302.

[15] M. Sisti, et al., **"New limits from the milano neutrino mass experiment with thermal microcalorimeters"**, *Nuclear Instruments and Methods in Physics Research Section A: Accelerators, Spectrometers, Detectors and Associated Equipment*, vol. 520, no. 13, no. 13, pp. 125–131, 2004, doi:10.1016/j.nima.2003.11.273.

[16] A. Nucciotti, E. Ferri and O. Cremonesi, **"Expectations for a new calorimetric neutrino mass experiment"**, *Astropart.Phys.*, vol. 34, pp. 80–89, 2010, doi:10.1016/j.astropartphys.2010.05.004, e-print: arXiv:0912.4638 [hep-ph].

[17] A. De Rujula and M. Lusignoli, **"Calorimetric measurements of 163holmium decay as tools to determine the electron neutrino mass"**, *Physics Letters B*, vol. 118, no. 46, no. 46, pp. 429–434, 1982, doi:10.1016/0370-2693(82)90218-0.

[18] A. de Rujula and M. Lusignoli, **"Single electron ejection in electron capture as a tool to measure the electron neutrino mass"**, *Nuclear Physics B*, vol. 219, no. 2, no. 2, pp. 277 – 301, 1983, doi:10.1016/0550-3213(83)90642-9.

[19] C.W. Reich and Balraj Singh, **"Nuclear data sheets for a = 163",** *Nuclear Data Sheets*, vol. 111, no. 5, no. 5, pp. 1211 – 1469, 2010, doi:10.1016/j.nds.2010.04.001.

[20] G. Audi, A.H. Wapstra and C. Thibault, **"The ame2003 atomic mass evaluation: (ii). tables, graphs and references",** *Nuclear Physics A*, vol. 729, no. 1, no. 1, pp. 337 – 676, 2003, doi:j.nuclphysa.2003.11.003.
The 2003 NUBASE and Atomic Mass Evaluations.

[21] A. Nucciotti, **"Statistical sensitivity of 163-Ho electron capture neutrino mass experiments",** 2014, e-print: `arXiv:1405.5060 [physics.ins-det]`.

[22] Massimiliano Galeazzi, Flavio Gatti, Maurizio Lusignoli, Angelo Nucciotti and Stefano Ragazzi, **"The Electron Capture Decay of 163-Ho to Measure the Electron Neutrino Mass with sub-eV Accuracy and Beyond",** *submitted to Physical Review D*, 2012, e-print: `arXiv:1202.4763 [physics.ins-det]`.

[23] L. Gastaldo et al., **"The Electron Capture 163Ho Experiment ECHo",** *Journal of Low Temperature Physics*, 2014, doi:10.1007/s10909-014-1187-4.

[24] Hans Meissner, **"Superconductivity of contacts with interposed barriers",** *Physical Review*, vol. 117, pp. 672–680, February 1960, doi:10.1103/PhysRev.117.672.

[25] Omid Noroozian et al., **"High-resolution gamma-ray spectroscopy with a microwave-multiplexed transition-edge sensor array"**, *Applied Physics Letters*, vol. 103, no. 20, no. 20, 2013, doi:http://dx.doi.org/10.1063/1.4829156.